

Figure 49 Frames from high-speed video of slap-down drop.

drop used heavier clevis pins which did not break on impact. However the upper turnbuckles buckled which caused them to become shorter so there was still considerable relative rotation between the two impact limiters, as evident in the video frames. Figure 50 shows the uppermost turnbuckle following the drop.

Using the video editing program, the elapsed time was estimated between initial impact and the instant when the cask c.g. reached zero vertical velocity. That time was 0.028 +/-0.004 seconds. Unlike the first two drops, the cask kinetic energy had not been completely dissipated at the zero velocity instant since there was still significant rotational velocity present. The resolution of this measurement (i.e. the time between frames) was 0.002 seconds.



Figure 50 Uppermost turnbuckle after the slap-down drop.

Figure 50 also shows how the wires from the in-cask accelerometers were crushed and cut by being pinched between the impact limiter and the cask. In this case the relative rotation between the impact limiters and the cask was sufficient to pinch the cables, in spite of the 1/8th-inch-diameter protective rods on either side of the cable. Figure 50 shows that the diametral clearance between cask and impact limiter has been increased to well over an inch by deformation of the impact limiter. In an undeformed impact limiter, this clearance is only about 1/4th inch. Fortunately, the cable fault did not occur until about 25 milliseconds after the end of the main acceleration event so the important data was recorded.

Following the impact of the higher impact limiter against the ground, the package rotated counterclockwise (in the view of Figure 49) and its mass center rose approximately 25 inches,

indicating that about 93.3 percent of the kinetic energy was dissipated. Figure 51 shows the highest point in the first bounce.

F 245 / 0.486 s / 1280*1024 / 500 fps / 250 us Shutter / 0.510 s Pre-Trig / Thu Mar 29 14:55:41.289



Figure 51 Highest point in the first bounce during the slap-down drop.

8.3 Pressure sensing film

Figure 52 shows the pressure sensing film removed after the slap-down drop. The pattern of pressure between the cask and impact limiter is quite similar to that from the side drop.



Figure 52 Pressure sensing film removed from the cask and impact limiters after the slap-down drop.

8.4 Deformation measurements

Table 5 shows the measured cask profile deviation from the design nominal before and after the slap-down drop. The conclusion from these was that no significant damage to the cask had occurred.

Table 5 Measurements of cask before and after the slap-down drop.

| Deviation | Cask state at measurement | |
|-----------|---------------------------|----------------------|
| | After side drop | After slap-down drop |
| | Before slap-down drop | |
| Maximum | 0.0053 | 0.0047 |
| Minimum | -0.0109 | -0.0105 |

Figure 53 shows the deformation suffered by the impact limiter that was on the higher end of the cask. Figure 54 shows overlays of the measured impact limiter profiles before and after the slap-down drop. The lower part of the figure shows how much the inner diameter of the impact limiter was deformed when it rotated relative to the cask on impact.



Figure 53 Damage to the impact limiter from the "slap-down" end of the cask.

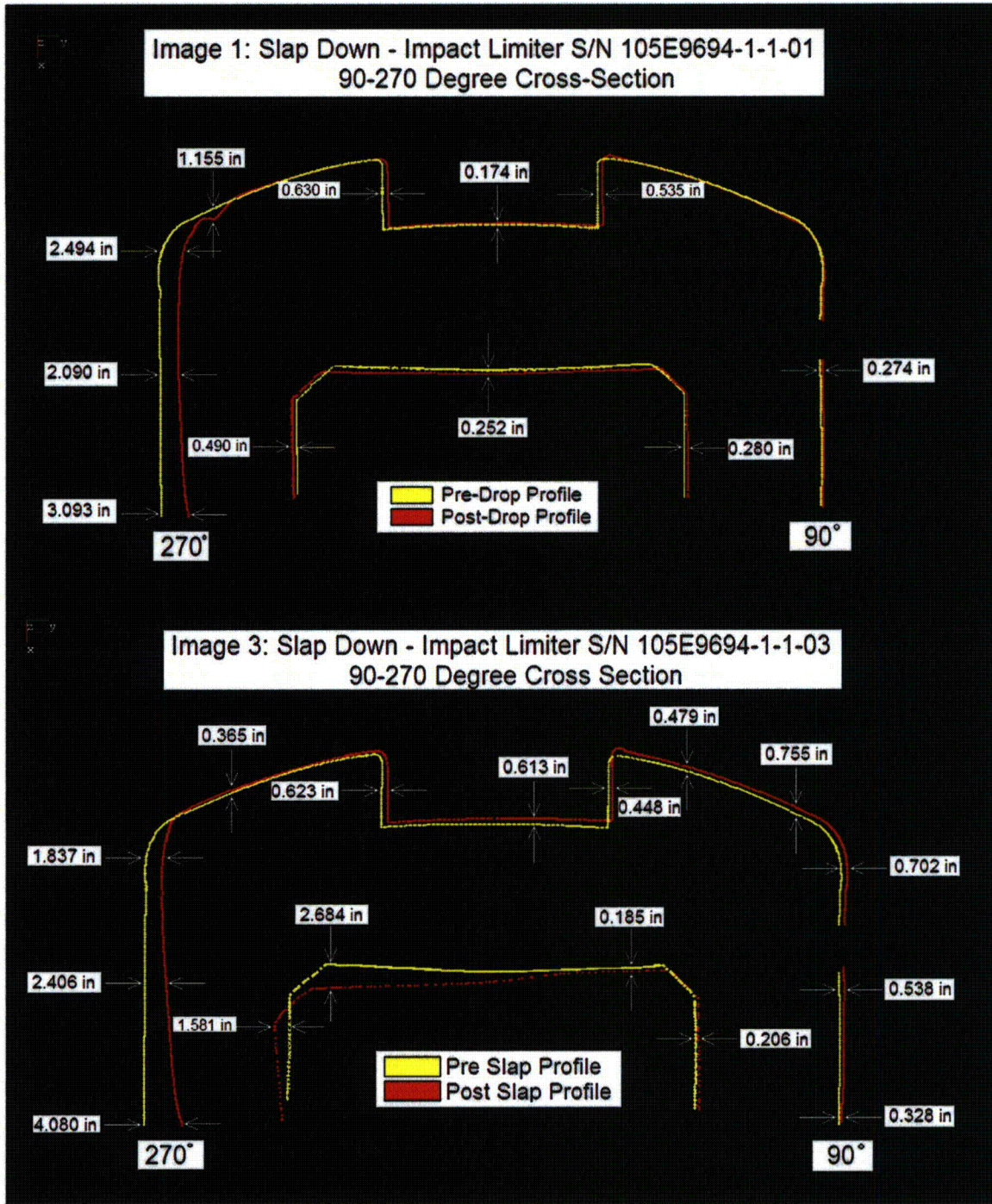


Figure 54 Profiles of the higher (top) and lower (bottom) impact limiters before and after the slap-down drop.

8.5 Leak rate test

The cask was leak tested following the slap-down drop and was found to meet specification. It was concluded that no degradation had occurred in the seal integrity of the cask.

9. Conclusions

The objectives, methods, and results of the drop test have been presented. The primary conclusions are as follows.

1. The cask and impact limiters passed the test. The cask passed its helium leak rate test before the first drop and after each of the three drops. No significant deformation of the cask was measured after any of the drops.
2. Measured peak accelerations are not usable for evaluating the accuracy of analytical predictions of cask and impact limiter behavior. Peak acceleration measured on the cask inner surface appears to be caused by secondary impacts between the internal tungsten shielding blocks and the steel cask body. The response to these impacts is not primarily dependent on impact limiter design.
3. Several measured acceleration time histories contained unexplained features. In particular, they did not exhibit a polarity consistent with the large decrease in downward velocity (i.e. upward acceleration) that had to exist at impact.
4. Two of the three drops caused accelerometers measuring in the vertical or near-vertical direction to exceed their 1000-g range. Therefore the waveform indicated by these accelerometers following the over-range is probably corrupted. The only conclusion that can be drawn from these data is that the peak acceleration exceeded 1000 g's at the sensor location. Acceleration data from the end drop is not over-ranged and should be accurate throughout the transient duration.
5. The high-speed video data allowed a reasonably accurate estimate to be made of the total elapsed time for deceleration of the cask c.g. from its impact velocity to zero. This data may be of use in evaluating the accuracy of the analytical predications.

THIS PAGE INTENTIONALLY LEFT BLANK

2.12.6.2 Free-Drop Test Activity Record – Pre- and Post-Leak Test

THIS PAGE INTENTIONALLY LEFT BLANK

AOS-165 TRANSPORT PACKAGE FREE DROP TEST ACTIVITY RECORD


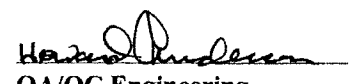
Step No. Activity Completed Date

.4.4 • Pre-test leak test performed (continue).
 Temp. of CL: 60° Temp. Corrected Leak Rate: _____
 Thermometer Type: Digital S/N: 1894 Cal. Due: 05/15/2007
TEST PARAMETERS:
 Tracer Gas: Helium Concentration of Cylinder welding grade 210348 USA 43.07
 Ambient Temp: 60°F Acceptance Criteria: 2.64 x 10⁻⁷ Cylinder ID: 102-227-5-HE-5
TEST RESULTS: (Seal Joint)
 Pre-Cal. Rate: 2.3 x 10⁻⁹ Leak Rate: 2.3 x 10⁻⁹ Post-Cal Rate: 2.4 x 10⁻⁹
 Test Results: Accept/Reject. Performer: R. P. Martin Level: III Cert. No. GE026
 COMMENTS: Tested Gasket only

TEST RESULTS: (Vent Port Plug)
 Pre-Cal. Rate: _____ Leak Rate: _____ Post-Cal Rate: _____
 Test Results: Accept/Reject. Performer: _____ Level: _____ Cert. No. _____
 COMMENTS: N/A Used Ranor, Inc. TEST RESULTS.

TEST RESULTS: (Drain Port Plug)
 Pre-Cal. Rate: _____ Leak Rate: _____ Post-Cal Rate: _____
 Test Results: Accept/Reject. Performer: _____ Level: _____ Cert. No. _____
 COMMENTS: N/A Used Ranor, Inc. TEST RESULTS

Additional Comments:

Activities Completed:  Project/Test Engineering  QA/QC Engineering

AOS-165 TRANSPORT PACKAGE FREE DROP TEST ACTIVITY RECORD

HBA 4-4-07
 96 HBR
 Page 167 of 17

Step No. Activity Completed Date

D.0 Post-Test - Orientation: END Drop Date: 3-19-07 Time: 8:00 AM

- .1 Videotape cameras stopped.
- .2 Acceleration signal tapes replayed.
- .3 Videotape replayed and package orientation at impact checked.
- .4 Still photos of package taken.
- .5 Impact limiter(s) removed and still photos of the package taken.
- .6 Pressure-sensing film removed, marked, and packed for safe storage.
- .7 Dimensional inspection of the cask and impact limiter(s) taken.
- .8 Pre-test leak test performed.

| | |
|-----|---------|
| 12P | 3/19/07 |
| 12P | 3/19/07 |
| 12P | 3/19/07 |
| 12P | 3/19/07 |
| 12P | 3/19/07 |
| 12P | 3/19/07 |
| 12P | 3/19/07 |
| 12P | 3/19/07 |
| 12P | 3/19/07 |
| 12P | 3/19/07 |
| 12P | 3/19/07 |
| 12P | 3/19/07 |

TEST EQUIPMENT:

MSLD: Mfr: ACATER Model: 180 t S/N: na
 Calibrated Leak (CL) S/N: 3437 Leak Rate: 2x61x10⁻⁷ Cal. Due: 11/02/2007
 Temp. of CL: 58° F C/F. Temp. Corrected Leak Rate:
 Thermometer Type: Digital Thermo Sta S/N: 1277 Cal. Due: 05/15/2007

TEST PARAMETERS:

Tracer Gas: Helium Concentration of Cylinder 99.99% Cylinder ID: 102-227-5-HE-5
 Ambient Temp: 61.5 C/F. Acceptance Criteria: 1.98 x 10⁻⁷

TEST RESULTS:

Pre-Cal. Rate: 2.3 x 10⁻⁹ Leak Rate 9 x 10⁻⁹ 10⁻⁹ 3/20/07 Post-Cal Rate: 2.3 x 10⁻⁹
 Test Results: Accept/Reject Performer: R. POMARCI Level: III Cert. No. C260

COMMENTS:

Activities Completed:

David A. Kienhof
 Project/Test Engineering

Howard D. Dineen
 QA/QC Engineering
BCA AOS QA

9 **COMMENTS:**

36 Rev. 3
 35 HBA 4.3.07

AOS-165 TRANSPORT PACKAGE FREE DROP TEST ACTIVITY RECORD

460444
Page 12-12 of 17

| Step No. | Activity | Completed | Date |
|----------|---|-----------|---------|
| D.0 | Post-Test - Orientation: <u>Side Drop</u> Date: <u>3/24/07</u> Time: <u>5:00P</u> | | |
| .1 | Videotape cameras stopped. | DAK | 3/24/07 |
| .2 | Acceleration signal tapes replayed. | DAK | 3/24/07 |
| .3 | Videotape replayed and package orientation at impact checked. | DAK | 3/24/07 |
| .4 | Still photos of package taken. | DAK | 3/24/07 |
| .5 | Impact limiter(s) removed and still photos of the package taken. <i>Remove one panel.</i> | DAK | 3/24/07 |
| .6 | Pressure-sensing film removed, marked, and packed for safe storage. | DAK | 3/24/07 |
| .7 | Dimensional inspection of the cask and impact limiter(s) taken. | DAK | 3/24/07 |
| .8 | Pre-test leak test performed. | WBA | 3/23/07 |

TEST EQUIPMENT:

MSLD: Mfr: varian Model: 979 S/N 6634016
 Calibrated Leak (CL) S/N: 3437 Leak Rate: 2.4 x 10⁻⁷ Cal. Due: 11-02-07
 Temp. of CL: 58.6 °C Temp. Corrected Leak Rate: 1.97 x 10⁻⁷
 Thermometer Type: Digital S/N: 1594 Cal. Due: 5-15-07

TEST PARAMETERS:

Tracer Gas: Helium Concentration of Cylinder welding grade 99.999% % Cylinder ID: 102-227-5-HE-5
 Ambient Temp: 41.4 °C Acceptance Criteria: 1.94 x 10⁻⁷

TEST RESULTS:

Pre-Cal. Rate: 1.97 x 10⁻⁷ Leak Rate: 2.3 x 10⁻⁸ Post-Cal Rate: 1.97 x 10⁻⁷
 Test Results: Accept/Reject. Performer: RP Level: HL Cert. No. 0260

COMMENTS:

Activities Completed:

[Signature]
Project/Test Engineering

[Signature]
QA/QC Engineering

.9 **COMMENTS:**

AOS-165 TRANSPORT PACKAGE FREE DROP TEST ACTIVITY RECORD

HBA 4/21/07
4-15
Page 17 of 17
KAP 4-4-07

Step No. Activity Completed Date

4.4 Pre-test leak test performed (continue).
Temp. of CL: 50.4 °C Temp. Corrected Leak Rate: _____
Thermometer Type: Digital S/N: 1894 Cal. Due: 5-15-2007
TEST PARAMETERS:
Tracer Gas: Helium Concentration of Cylinder Welding Grade % Cylinder ID: 162-227-5-HE-5
Ambient Temp: 41.4 °C Acceptance Criteria: _____
TEST RESULTS: (Seal Joint)
Pre-Cal. Rate: 2.5 x 10⁻⁹ Leak Rate 2.3 x 10⁻⁸ Post-Cal Rate: 2.5 x 10⁻⁹
Test Results: Accept/Reject. Performer: RJP Level: III Cert. No. 0260
COMMENTS: _____

TEST RESULTS: (Vent Port Plug)
Pre-Cal. Rate: 2.5 x 10⁻⁹ Leak Rate 2.1 x 10⁻⁸ Post-Cal Rate: 1.3 x 10⁻⁶
Test Results: Accept/Reject. Performer: RJP Level: III Cert. No. 0260
COMMENTS: _____

TEST RESULTS: (Drain Port Plug)
Pre-Cal. Rate: 2.5 x 10⁻⁹ Leak Rate 2.3 x 10⁻⁸ Post-Cal Rate: 2.5 x 10⁻⁶
Test Results: Accept/Reject. Performer: RJP Level: III Cert. No. 0260
COMMENTS: _____

Additional Comments:

Post processing with 15 psi Helium for five (5) minutes with no leakage.

Pressure gauges used S/N 003 and S/N 004 were calibrated week 33 of 2006 and due due for calibration week 33 of 2007.

Activities Completed:

R. POMARCI
Project/Test Engineering

Harold Anderson
QA/QC Engineering

2.12.7 Dimensional Inspection Report

THIS PAGE INTENTIONALLY LEFT BLANK

RANOR / GE Energy / AOS
AOS-165 Cask Drop Test
Dimensional Summary Report No. 109699-01 (4-23-07)

RANOR Purchase Order No.: 109699

Part Names: AOS-165 Cask Assembly and Impact Limiters
Document References: Drawing Nos.105E9692 Rev. 2; 105E9694 Rev. 3;
Specification No. 22A9418 Rev. 3
Serial Numbers: AOS-165 105E9693-1 (RANOR S/N 050280-01)
AOS-165 105E9694-1-1-01 (RANOR S/N 060452-01)
AOS-165 105E9694-1-1-02 (RANOR S/N 060452-02)
AOS-165 105E9694-1-1-03 (RANOR S/N 060452-03)
AOS-165 105E9694-1-1-04 (RANOR S/N 060452-04)
AOS-165 105E9694-1-1-05 (RANOR S/N 060452-05)
Inspection Dates: March 16-30, 2007
Attachments: FARO Calibration Certificate No. 4655 (10-19-2006)

Inspection Conditions:
Location: GE Nuclear Energy Vallecitos Nuclear Center Sunol, CA 95486
Material: Stainless Steel
Measurement Units: Inches

East Coast Metrology was contracted by RANOR, Inc. for performance of On-Site Laser Tracker Inspection Services of the AOS-165 Cask Assembly and Impact Limiters fabricated by RANOR. The items were located at GE Nuclear Energy Vallecitos Nuclear Center 6705 Vallecitos Road Sunol, CA 95486.

East Coast Metrology utilized a FARO Laser Tracker Model X System, Serial No. X01000601930 for performing the dimensional inspections. The equipment has been calibrated by the manufacturer - FARO Technologies Kennett Square, PA 19348 on October 18, 2006, calibration due October 18, 2007 (FARO Calibration Certificate Number 4655) using standards traceable to the National Institute of Standards and Technology (NIST).

All dimensional inspection was performed under the direction and observation of GE Nuclear Energy Raul Pomares, Project Manager for the AOS-165 Cask Assembly and components.

The AOS-165 Cask Assembly and accompanying Impact Limiters were inspected by *East Coast Metrology* before and after each drop test to determine the extent of deformation due to each type of drop. Each component was scanned and compared to its corresponding CAD model using a Laser Tracker. See the following for a summary of the inspections and data.

AOS-165 Cask Assembly:

For each set of scan data for the Cask, the 0, 90, 180, and 270 degree profiles were scanned. An alignment using the axis of the cylindrical part of the cask as the controlling datum was used. This axis was then intersected with the "Lid End" of the Cask and a point was constructed. Another point was measured at the 90 degree lifting lug to establish the other axis. This alignment was repeated for each measurement of the Cask.

The table below, *Table 1*, shows the maximum and minimum deviations of the profiles of the Cask when compared to its CAD model for each drop test. The maximum (positive) deviations indicate the profile of the Cask was larger than that of the model. Similarly, the minimum (negative) deviations indicate that the profile of the Cask was smaller than that of the model.

Table 1: Cask Assembly Pre- and Post- Drop Profile Deviations from CAD Model (inches)

| Cask Condition | Pre End Drop | Post End Drop | Post Side Drop | Post Slap Down |
|-------------------|--------------|---------------|----------------|----------------|
| Maximum Deviation | 0.0068 | 0.0046 | 0.0053 | 0.0047 |
| Minimum Deviation | -0.0094 | -0.0101 | -0.0109 | -0.0105 |

Over the course of all three drop tests, the maximum deviations varied by a total of 0.0022 inches, while the minimum deviations varied by a total of 0.0015 inches. This indicates that the effect of the drop tests had a negligible impact on the profile of the Cask.

Below is a sample of the Cask profile from the Pre- End Drop scan. There are 2 pictures, *Image A* is the 0-180 Cross-Section of the Cask, and *Image B* is the 90-270 Cross-Section. The red areas represent the positive (maximum deviations) and the yellow areas represent the negative (minimum deviations).

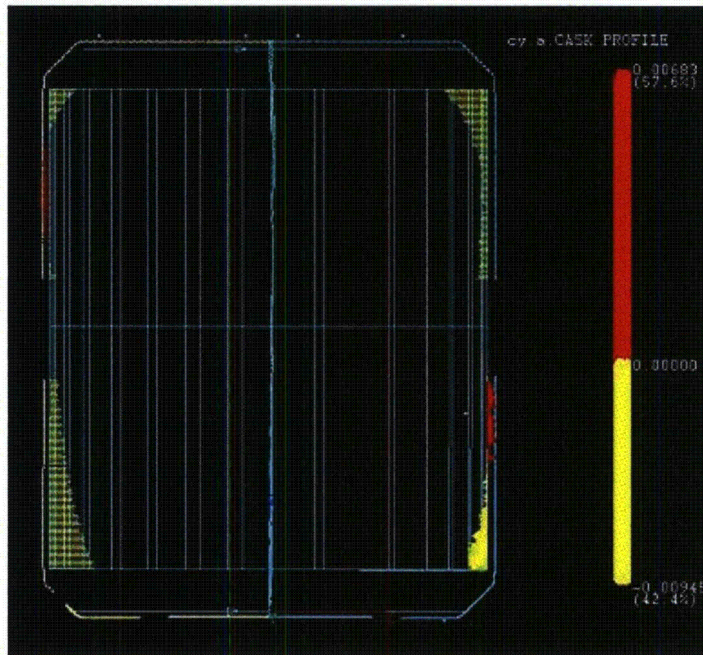


Image A: Cask Assembly Pre-End Drop Scan Data, 0-180 Degree Cross-Section

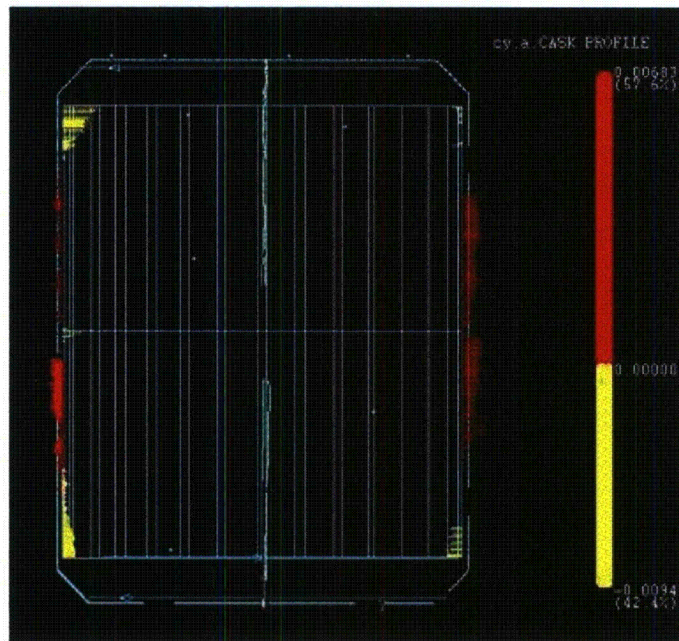


Image B: Cask Assembly Pre-End Drop Scan Data, 90-270 Degree Cross-Section

AOS-165 Cask Impact Limiter Assemblies:

For the Impact Limiters, scan data was taken at the 0, 30, 60, 90, 120, 150, 180, 210, 240, 270, 300 and 330 degree profiles. In order to compare each impact limiter in its pre- and post-drop condition, an alignment using the bottom perimeter (opposite the domed-end), measured as a circle, was used as a reference. By measuring it as a circle, the center point and vector of the measured circle were established. The portions of this circle that were deformed due to each drop test were not used in this calculation. The vector of this axis was defined to be the primary datum in this alignment. A point was then measured at the 90 degree lifting lug to establish the second axis in the coordinate system. This process provided the only repeatable means to align each impact limiter and subsequently compare the results.

Once the pre- and post-drop scan data was collected for each Impact Limiter, the 90-270 degree profile cross-sections were overlaid in order to calculate the magnitude of deformation for each drop. In the images below, each Impact Limiter has been analyzed in this manner and the deformations reported. They are listed below in the same order that the drop tests occurred: End Drop (Impact Limiter 5), Side Drop (Impact Limiters 1 & 3) and Slap Down (Impact Limiters 2 & 4).

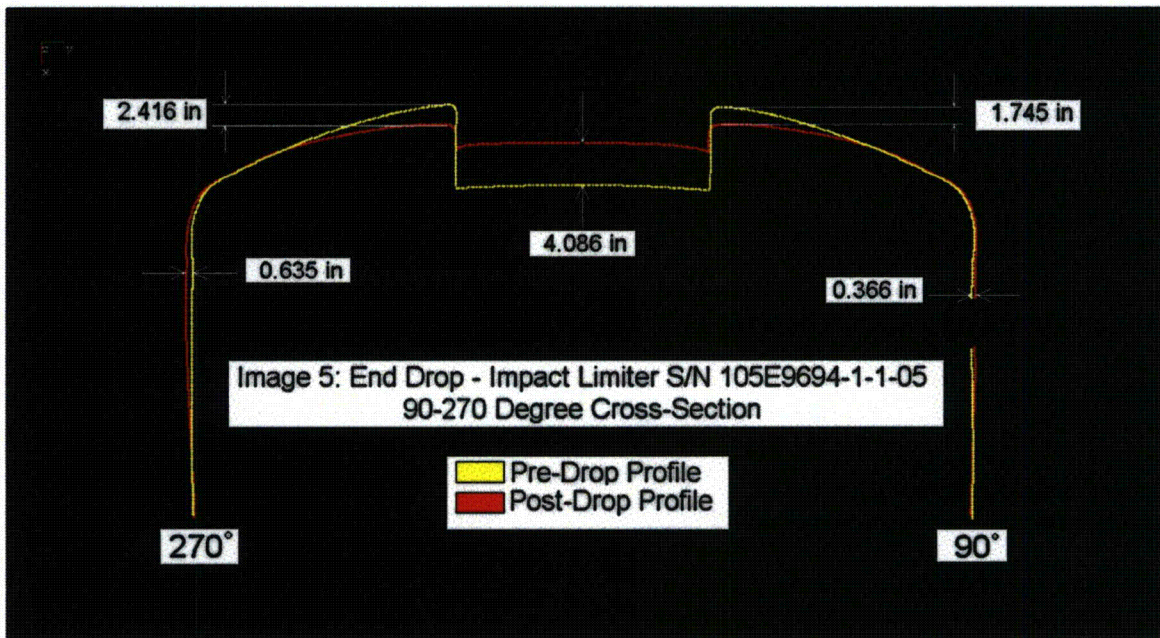


Image 5: Impact Limiter Serial No. 105E9694-1-1-05 - End Drop Cross-Section Overlay

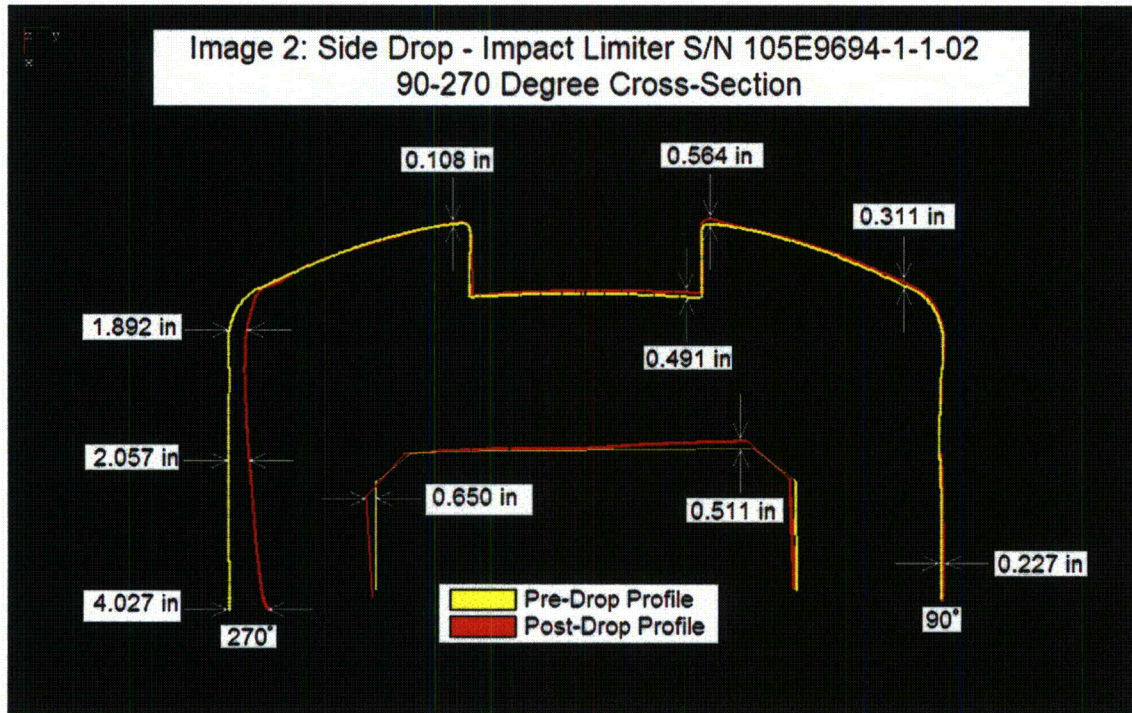


Image 2: Impact Limiter Serial No. 105E9694-1-1-02 - Side Drop Cross-Section Overlay

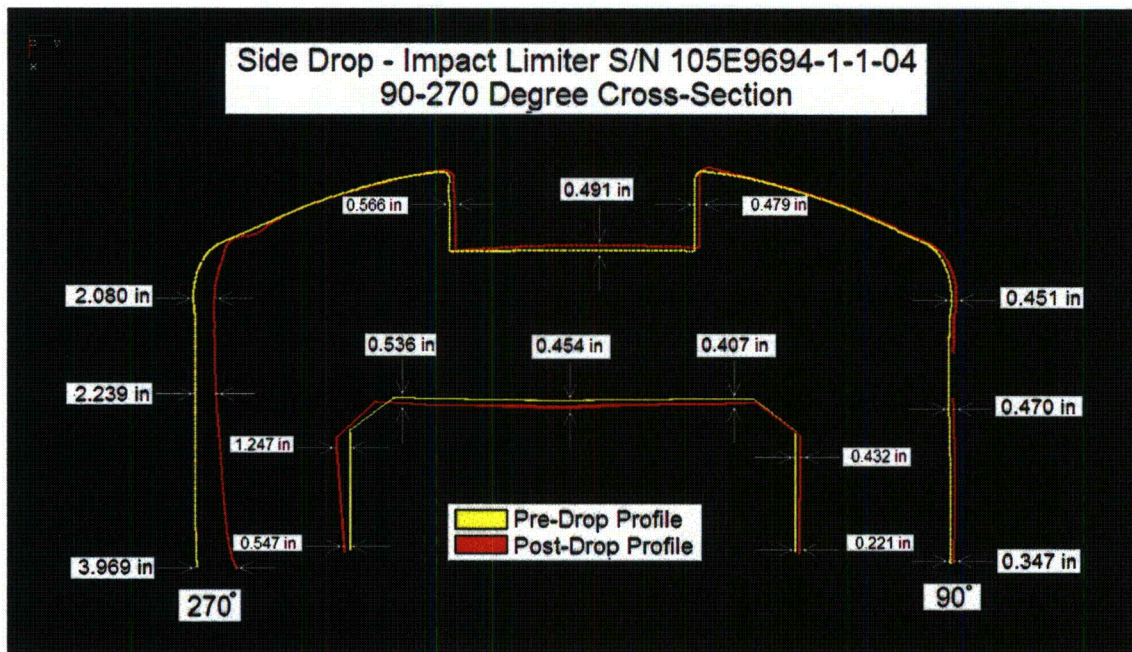


Image 4: Impact Limiter Serial No. 105E9694-1-1-04 - Side Drop Cross-Section Overlay

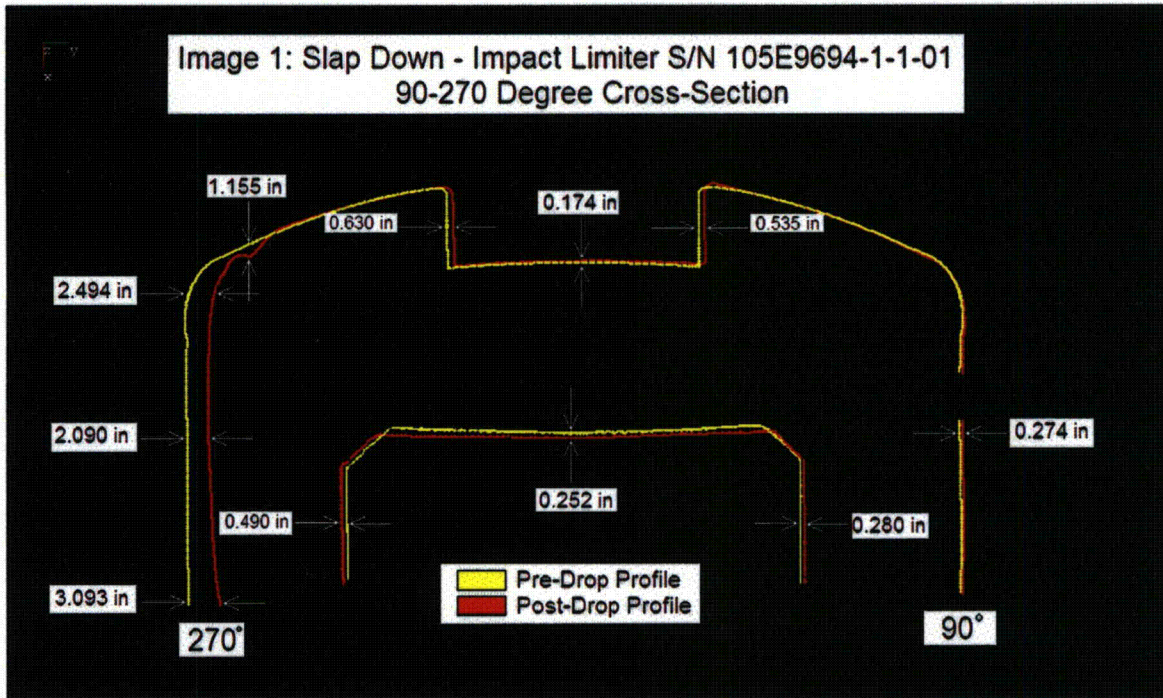


Image 1: Impact Limiter Serial No. 105E9694-1-1-01 - Slap Down Cross-Section Overlay

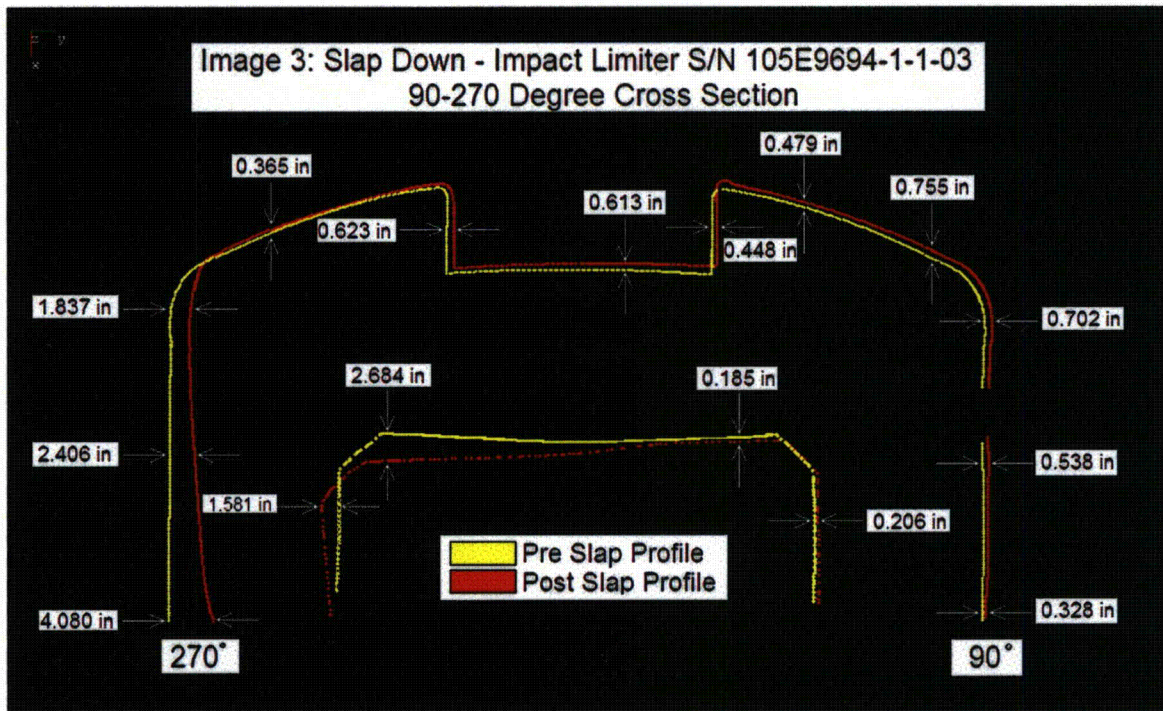


Image 3: Impact Limiter Serial No. 105E9694-1-1-03 - Slap Down Cross-Section Overlay



461 Boston Street ♦ Topsfield, Massachusetts 01983 ♦ Tel: 978-887-5781 ♦ Fax: 978-887-5782 ♦ www.EastCoastMetrology.com

Contact Information

As part of this report, *East Coast Metrology* appreciates the request for any additional information, which will help our customers find solutions to their measurement problems.

We proudly consider ourselves as allied partners to our customers, and can assist in the positioning and alignment of features, along with our ability to perform high accuracy measurements.

The key to our success is to be able to provide our customers with complete solutions, and the information that is most valuable to their cause, in a clear and concise manner.

We welcome any questions you may have, and look forward to working together in the near future.

Please feel free to contact us for additional information or concerns that may arise.

David K. Kramer
Project Engineer
East Coast Metrology
461 Boston Street (A4)
Topsfield, Massachusetts 01983
Tel: 503.997.7055
Fax: 603.251.5678
E-mail: dkramer@eastcoastmetrology.com

Attachments:

AOS-165 Cask Assembly Impact limiter, Serial No. 105E9694-1-1-01 Pre- and Post- Slap Down Scan Data (12 pgs)
AOS-165 Cask Assembly Impact limiter, Serial No. 105E9694-1-1-02 Pre- and Post- Side Drop Scan Data (10 pgs)
AOS-165 Cask Assembly Impact limiter, Serial No. 105E9694-1-1-03 Pre- and Post- Slap Down Scan Data (14 pgs)
AOS-165 Cask Assembly Impact limiter, Serial No. 105E9694-1-1-04 Pre- and Post- Side Drop Scan Data (12 pgs)
AOS-165 Cask Assembly Impact limiter, Serial No. 105E9694-1-1-05 Pre- and Post- Head Drop Scan Data (10 pgs)

RANOR/GE/AOS
Report No. 109699-01

AOS-165 Cask Drop Test Dimensional Summary Report
Page 7 of 7

RANOR P.O. No. 109699
Date: 4/23/2007

THIS PAGE INTENTIONALLY LEFT BLANK

2.12.8 Analysis of Content-Cask Lid Impact

Content accelerations due to head-on 30-ft. package drops and content-cask lid gaps are determined by equating impact kinetic energy to strain energy within the impact limiter. The cask and impact limiter are modeled as a generalized single degree of freedom (SDOF) spring-mass system, using an approximation of the impact limiter force-displacement relation determined in the 30-ft. drop analyses. The content is also modeled as a generalized lumped mass, and content impact kinetic energy determined from a central impact formulation. The velocities applied in the central impact calculation are determined from equations of motion for the two generalized masses under gravitational force and initial velocity.

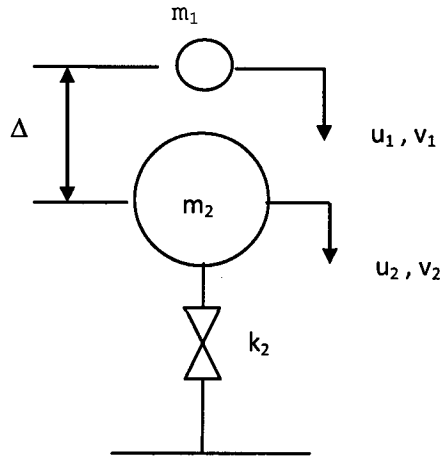


Figure 2-68. Generalized Model of Impact I

| | | | | | |
|-------|---|---------------------------------|----------|---|---------------------------------|
| a | = | Content acceleration | T | = | Kinetic energy |
| e | = | Coefficient of restitution | U | = | Strain energy |
| g | = | Gravitational acceleration | v_0 | = | Initial velocity |
| k | = | Impact limiter spring stiffness | v_1 | = | Content velocity |
| m | = | Effective mass | v_2 | = | Cask velocity |
| m_1 | = | Content mass | w_1 | = | Content weight |
| m_2 | = | Package mass | w_2 | = | Package weight |
| P | = | Impact force | δ | = | Spring displacement |
| u_1 | = | Content displacement | Δ | = | Gas |
| u_2 | = | Cask displacement | ω | = | Frequency, $\sqrt{(k_2 / m_2)}$ |

Content equation of motion for initial velocity v_0 and force g :

$$g = d^2u_1 / dt^2$$

$$u_1 = g * t^2 / 2 + v_0 * t$$

$$v_1 = du_1 / dt = g * t + v_0$$

Cask equation of motion for initial velocity v_0 and force g :

$$g = d^2u_2 / dt^2 + (k_2 / m_2) * u_2$$

$$\omega = \sqrt{(k_2 / m_2)}$$

$$u_2 = (v_0 / \omega) * \sin \omega t + g * t^2 / 2$$

$$v_2 = du_2 / dt = v_0 * \cos \omega t + g * t$$

for, $\sin \omega t = \omega t - (\omega t)^3 / 6,$

$$u_2 = (v_0 / \omega) * [\omega t - (\omega t)^3 / 6] + g * t^2 / 2$$

$$u_2 = v_0 * t - v_0 * \omega^2 t^3 / 6 + g * t^2 / 2$$

Equating cask and content displacements:

$$\Delta = u_1 - u_2$$

$$= v_0 * \omega^2 * t^3 / 6$$

$$t = (6 * \Delta) / (v_0 * \omega^2)^{1/3}$$

Impact kinetic energy:

$$T = 0.5 (1 - e^2) * (v_2 - v_2)^2 * [m_1 * m_2 / (m_1 + m_2)]$$

$$m = [m_1 * m_2 / (m_1 + m_2)]$$

$$e = 0.0$$

$$T = 0.5 * m * (v_1 - v_2)^2$$

$$= 0.5 * m * v_0^2 * (1 - \cos \omega t)^2$$

Equating strain and kinetic energy:

$$\begin{aligned} T &= k \cdot \delta^2 / 2 \\ \delta &= \sqrt{(2 \cdot T / k)} \\ P &= k \cdot \delta = \sqrt{(2 \cdot T \cdot k)} \\ a &= P / w_1 = \sqrt{(2 \cdot T \cdot k)} / w_1 \end{aligned}$$

Applying equations to AOS casks:

| Model | W1 (lb) | W2 (lb) | K (lb/in) | Gap (in) | Freq (hz) | Acc (g) |
|---------|-----------|-----------|-----------|-----------|-----------|-----------|
| ----- | ----- | ----- | ----- | ----- | ----- | ----- |
| AOS-025 | 1.500E+01 | 1.680E+02 | 1.390E+05 | 1.000E-01 | 8.999E+01 | 8.662E+02 |
| AOS-050 | 6.000E+01 | 1.181E+03 | 1.040E+05 | 1.000E-01 | 2.936E+01 | 1.868E+02 |
| AOS-100 | 5.000E+02 | 9.510E+03 | 2.330E+05 | 5.000E-01 | 1.549E+01 | 1.798E+02 |

Fortran program for equation evaluation (ContentAcc.for):

```
c
c   a   - content acceleration in g
c   f   - package frequency
c   g   - gap
c   xk  - impact limiter stiffness
c   xm  - effective mass
c   xm1 - content mass
c   xm2 - package mass
c   t   - time to contact
c   T   - 2x kinetic energy
c   v0  - initial velocity
c   w1  - content weight
c   w2  - package weight
c
c       implicit real*8 (a-h,o-z)
c
c   open files & initialize output
c       open(1,file='contentacc.in')
c       open(2,file='contentacc.out')
c       write(2,'(5x,5hModel,5x,6hW1(1b),5x,6hW2(1b),3x,8hK(1b/in),
c &         4x,7hGap(in),3x,8hFreq(hz),5x,6hAcc(g))')
c       write(2,'(5x,5h-----,5x,6h-----,5x,6h-----,3x,8h-----,
c &         4x,7h-----,3x,8h-----,5x,6h-----)')
c
c       initialize constants
c       v0=527.5
c       exp=0.333333
c       pi2=6.28319
c
c   loop on models
c   do n=1,3
c       read(1,*) model,w1,w2,xk,g
c       xm1=w1/386.4
c       xm2=w2/386.4
c       xm=xm1*xm2/(xm1+xm2)
c       f=dsqrt(xk/xm2)
c       t=(6*g/(v0*f**2))**exp
c       T=xm*v0**2*(1-dcos(f*t))**2
c       a=dsqrt(T*xk)/w1
c       write(2,'(i10,6es11.3)') model,w1,w2,xk,g,f/pi2,a
c   enddo
c
c       end
```

Input data (ContentAcc.in):

```
100,500,9510,2.33e5,0.5
50,60,1181,1.04e5,0.1
25,15,168,1.39e5,0.1
```

2.12.9 Comparison of Libra Static and Dynamic Impact Analysis

Date February 9, 2010

Libra static and dynamic impact analyses are compared to assess applicability of the static method to AOS cask drop analyses. Results of static and dynamic analyses of a 30-ft. head-on drop are compared. A model 165 cask with 20 psf density foam is used in the analyses. Both impact forces and displacements given by the two solutions are shown to be in good agreement.

In the Libra dynamic analysis, the impact velocity corresponding to a 30-ft. drop is applied as an initial condition, and cask response is determined by a direct integration solution. An axisymmetric, 2D model of the foam and cask is used. The FEA model is shown in [Figure 2-69](#), where the foam and cask are distinguished by different colors. The cask is modeled as a solid steel cylinder, with density adjusted to give a total cask and foam weight of 40k. A bi-linear foam constitutive model and von Mises yield criteria is used, with initial modulus of 19.0 ksi, secondary modulus of 5.4 ksi, and an equivalent yield stress of 2.0 ksi. The initial modulus and yield stress are based on foam stress at 10% strain, and the secondary modulus is based on the foam stress at 10% and 65% strains. Both foam to ground and foam to cask interfaces are modeled by gapped, compression-only, spring elements.

Cask time-history displacement determined in the dynamic analysis is shown in [Figure 2-70](#). The maximum displacement is 5.76 in, and occurs at 0.016 sec. Forces in ground impact springs are shown in [Figure 2-71](#) and [Figure 2-72](#). [Figure 2-71](#) shows forces in individual ground contact springs, while [Figure 2-72](#) shows the resultant of all ground contact springs. In [Figure 2-71](#), time lapses before springs compress reflect developing foam-ground contact. From [Figure 2-72](#), the maximum, total impact force is 6020 k. The deformed model at maximum displacement is shown in both [Figure 2-73](#) and [Figure 2-74](#). [Figure 2-73](#) shows only the foam deformation, while [Figure 2-74](#) shows both the foam and cask deformation, with displacement contours super-imposed.

Libra static drop analyses involve determining impact force and foam strain energy due to deformation at ground contact locations. Maximum impact force corresponds to the value of strain energy equal to the potential energy of the 30-ft. drop. A 180°, 3D foam model, shown in [Figure 2-75](#), is used in the analysis. Results of the static analysis are shown in [Figure 2-76](#) and [Figure 2-77](#). [Figure 2-76](#) shows the deformed model at maximum displacement, while [Figure 2-77](#) shows force and energy developed in the analysis. For a 180° model, the required strain energy is half the potential energy of a 40 k structure drop, or 7200 in-k. From [Figure 2-77](#), the corresponding displacement is 5.7 in, and the impact force is 6400 k. [Figure 2-77](#) is based on an accurate foam constitutive model. A static analysis is also performed using the approximate bi-linear foam constitutive model applied in the dynamic analysis. Plots of force and energy for the bi-linear constitutive model are presented in [Figure 2-78](#), and the impact force is 6800 k.

The 5.7 in displacement and 6400 k force determined in the static analysis from [Figure 2-77](#) compare well to the 5.76 in displacement and 6020 k force determined in the dynamic analysis. In addition, the deformation patterns given by the two solutions are also in good agreement. For the same constitutive model, the static method gives 6800 k while the dynamic method gives 6020 k, indicating the static method is conservative.

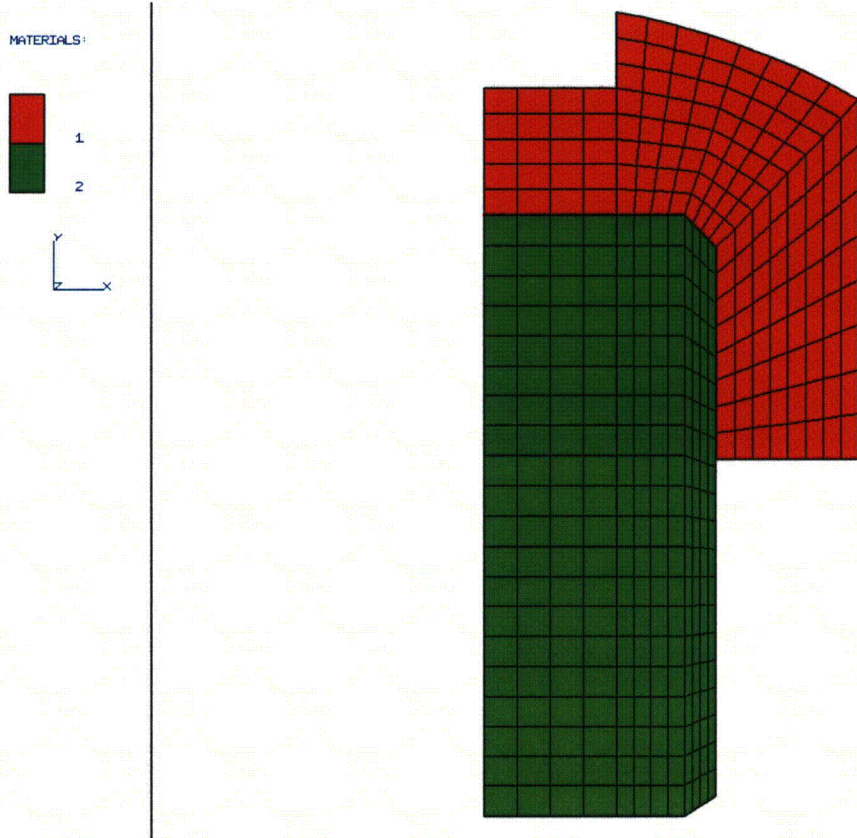


Figure 2-69. Dynamic Analysis FEA Model

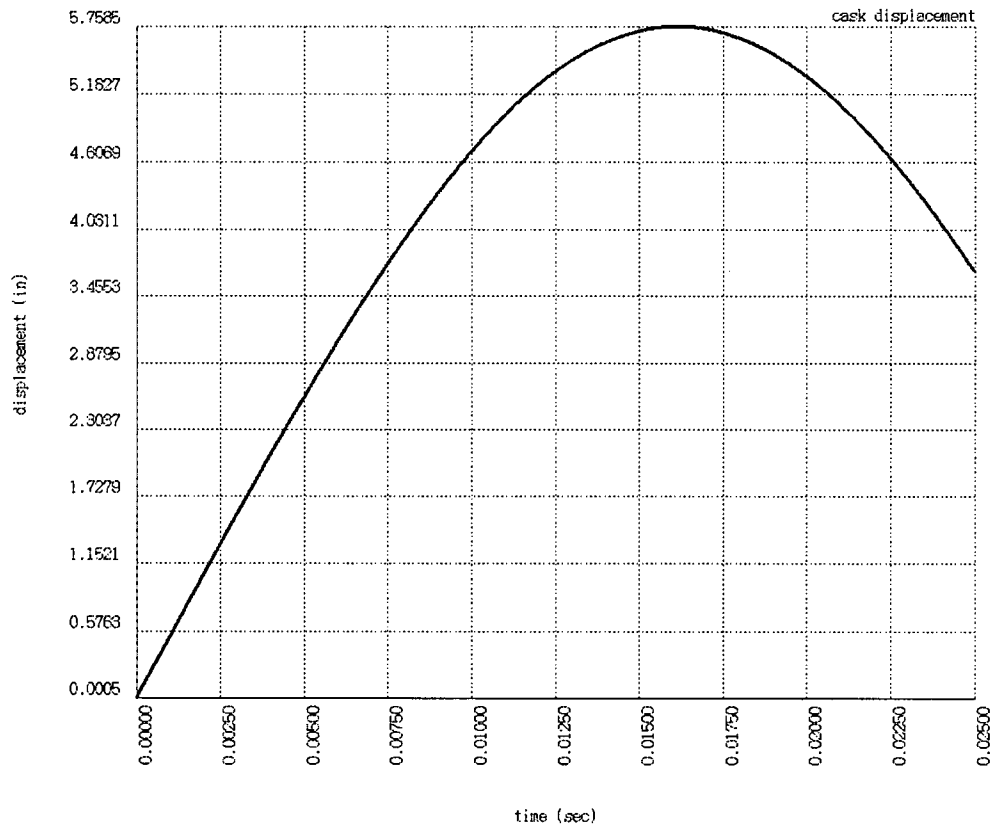


Figure 2-70. Cask Displacement Time-History

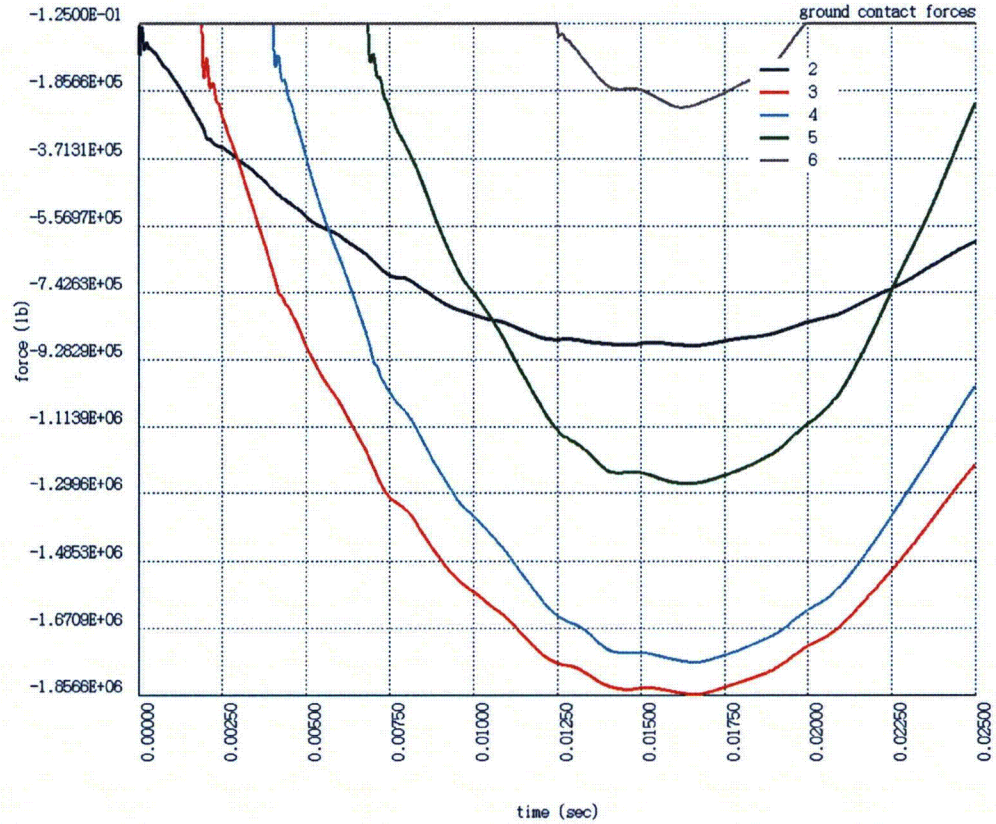


Figure 2-71. Ground Impact Forces in Dynamic Model

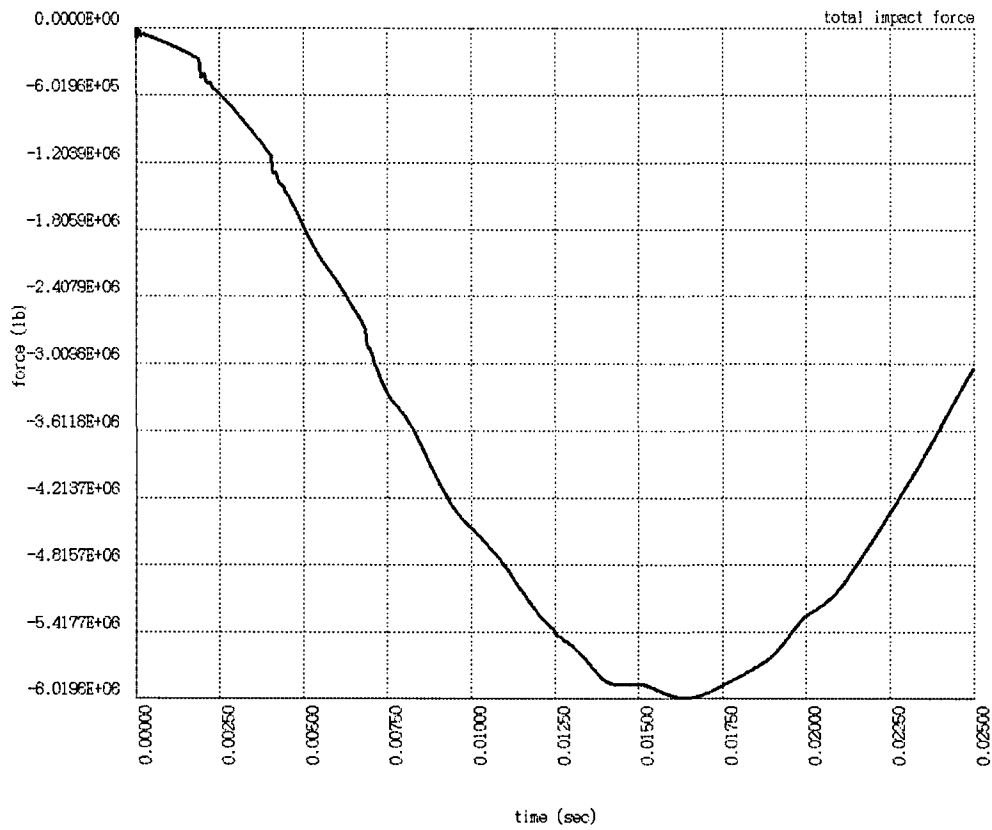


Figure 2-72. Total Ground Impact Force in Dynamic Model

```

VEC: 16
AMPL: 1.0
SQUARE OFF
SCALE: 0.95

BOUNDARIES:
X: 0.000
  37.500
Y: -43.000
  37.700
Z: 0.000
  0.000

```

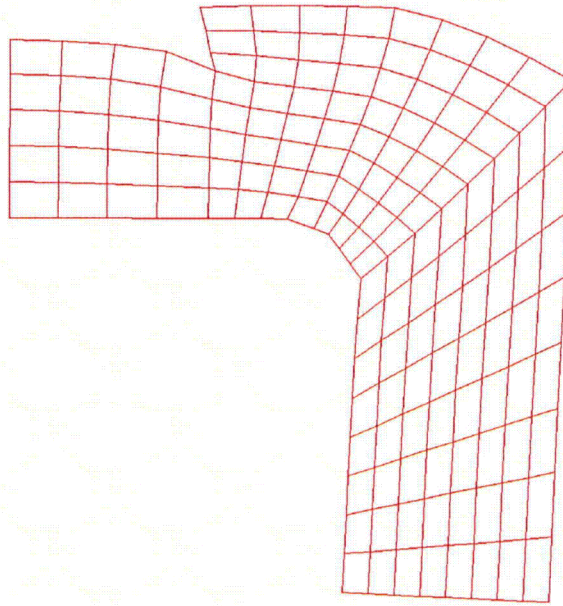


Figure 2-73. Deformed Dynamic Model at Maximum Displacement

```

VECTOR: 16
DOF: 2
MIN: 8.8874E-02
MAX: 5.7603E+00

```

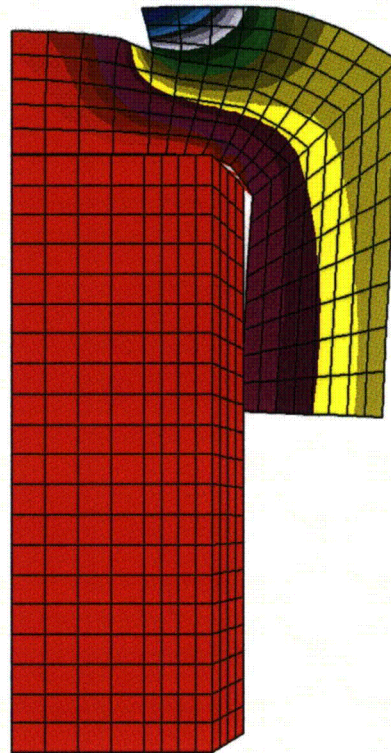
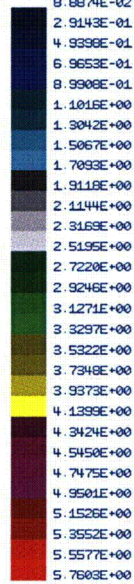


Figure 2-74. Displacement Contours n Deformed Dynamic Model

VEC: 0
AMPL: 0.000E+00
SQUARE: OFF
SCALE: 0.95

BOUNDARIES:
X: -37.500
37.500
Y: -8.000
35.700
Z: 0.000
37.295

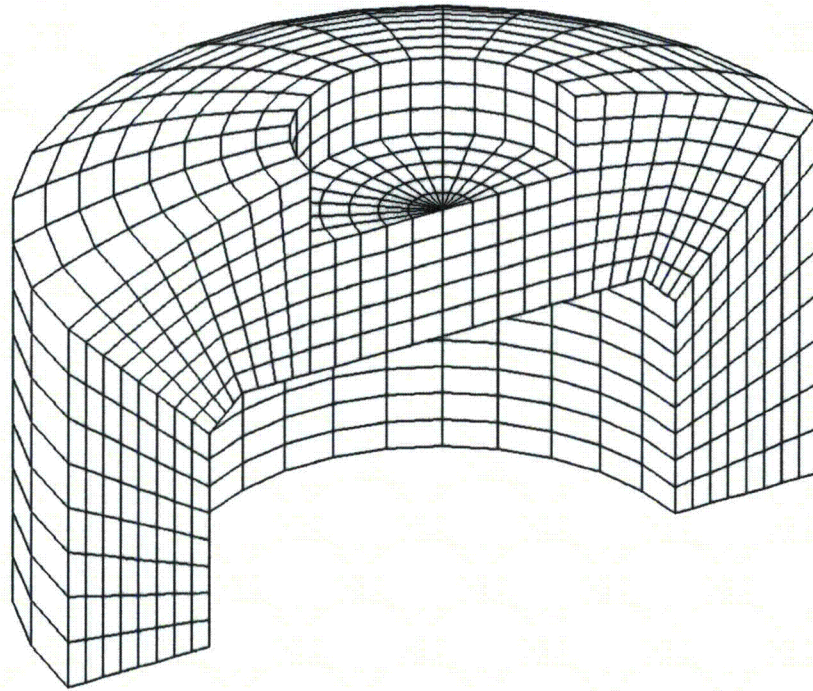


Figure 2-75. Foam Static Analysis FEA Model

VEC: 550
AMPL: 1.0
SQUARE: OFF
SCALE: 0.95

BOUNDARIES:
X: -37.500
37.500
Y: -8.000
35.700
Z: 0.000
37.295

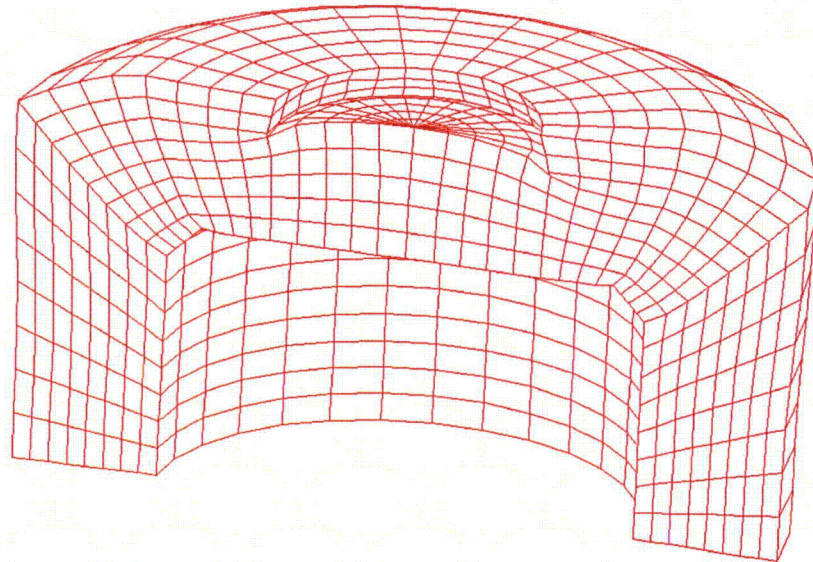


Figure 2-76. Deformed Foam Static Model at Maximum Displacement

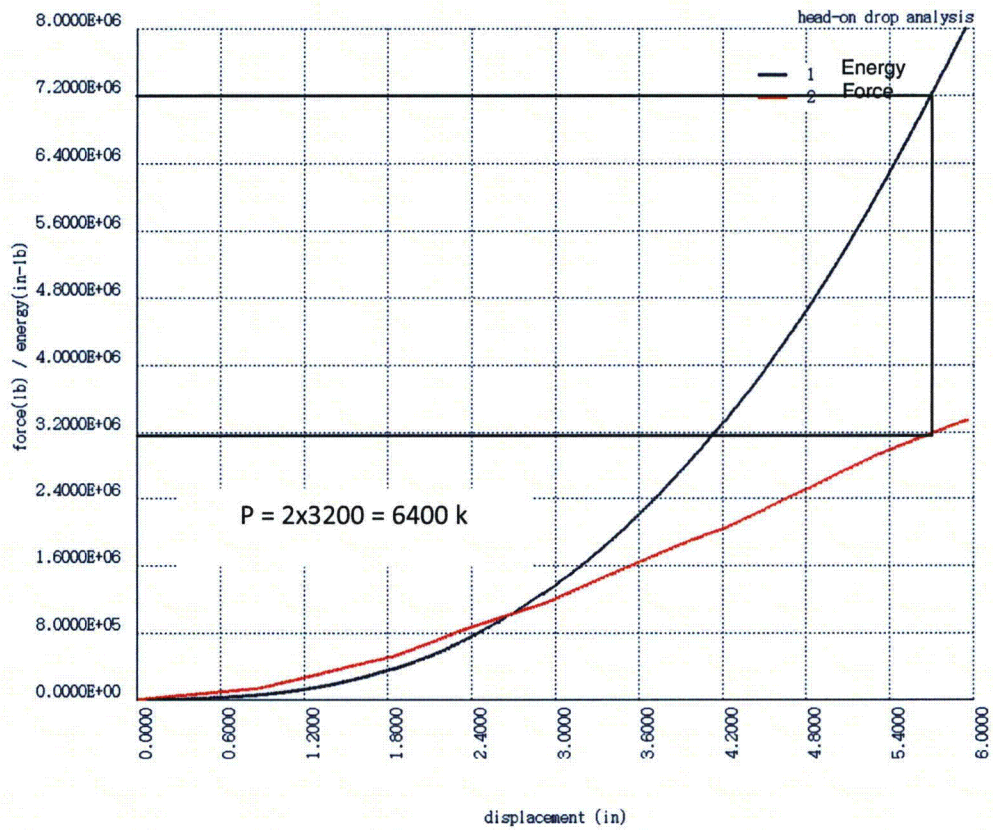


Figure 2-77. Energy and Force Plots for Static Analysis

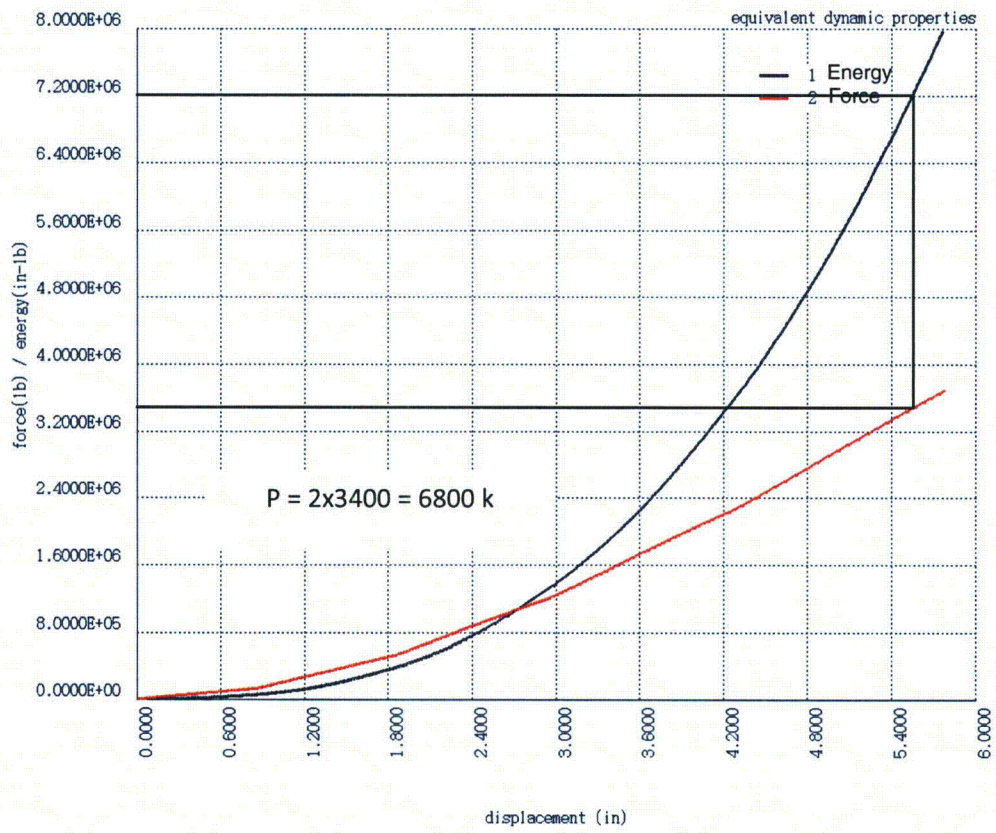


Figure 2-78. Energy and Force Plots for Static Analysis with Bi-Linear Stress-Strain

2.12.9.1 Appendix A – Libra Dynamic Impact Analysis Input File

ti dynamic impact analysis

*

mc 9

*

cnd 1, 23.3,-8,0
, 2, 37.5,-8,0
, 3, 37.5,27.9,0
, 4, 23.3,13.3,0
, 5, 20.1,16.5,0
, 6, 25.6,33.4,0
, 7, 13.3,36.7,0
, 8, 13.3,29.125,0
, 9, 0.0,16.5,0
, 10, 0.0,29.125,0
, 11, 19.4,35.3,0
, 12, 31.7,30.9,0
, 13, 13.3,16.5,0

*

* foam

*

g10

9,9, 1,1, 8,1, 0,1
1,2,3,4
-1

*

g10

9,5
4,3,6,5
6, 12
-1

*

g10

9,5
5,6,7,13
6, 11
-1

*

g10

5,6
9,13,8,10
-1

*

* pseudo cask

*

g10

5,21, 1001,1001, 8,2, 0,0
0,-43.6,0, 13.3,-43.6,0
13.3,16.4,0, 0,16.4,0
-1

*


```

g10  5,21, 1201,1201,  8,2, 0,0
      13.3,-43.6,0,  20.1,-43.6,0
      20.1,16.4,0,  13.3,16.4,0
      -1
*
g10  5,21, 1401,1401,  8,2, 0,0
      20.1,-43.6,0,  23.2,-41.6,0
      23.2,13.2,0,  20.1,16.4,0
      -1
*
* cask contact springs
*
el  2001,1,3, 1101,172,  4,1,1
,   2005,1,3, 1105,163
,   2006,1,3, 1302,154
,   2007,1,3, 1303,145
,   2008,1,3, 1304,136
,   2009,1,3, 1502,109
,   2010,1,3, 1503,100
,   2011,1,3, 1504,91
,   2012,1,3, 1505,73
*
* boundary contact springs
*
nd  3162, 16.3375, 36.7, 0
,   3153, 19.4, 36.7, 0
,   3144, 22.4875, 36.7, 0
,   3126, 25.6, 36.7, 0
,   3117, 28.6875, 36.7, 0
,   3108, 31.7, 36.7, 0
,   3171, 13.3, 37.7, 0
*
el  3001, 1, 4, 162,3162
,   3002, 1, 5, 153,3153
,   3003, 1, 6, 144,3144
,   3004, 1, 7, 126,3126
,   3005, 1, 8, 117,3117
,   3006, 1, 9, 108,3108
,   3007, 1,10, 171,3171
*
* merge nodes
*
me  0.001
*
* boundary cond
*
bc  3108,8,9, 12,0.0
*
* element properties
*
pr  1,101
,   101, 1.9e4,0.3,1.0e-6,3.0e-5,2.0e3,5.4e3

```

```

PR 2,102
, 102, 28.0E6,0.3,1.0E-5,0.00099,1.0e6,1.0e9
pr 3, 1.0e7,1.0e7,1.0e9, 1,0.0000,0, 0,0
pr 4, 1.0e7,1.0e7,1.0e9, 1,0.6375,0, 0,0
pr 5, 1.0e7,1.0e7,1.0e9, 1,1.4000,0, 0,0
pr 6, 1.0e7,1.0e7,1.0e9, 1,2.2875,0, 0,0
pr 7, 1.0e7,1.0e7,1.0e9, 1,3.3000,0, 0,0
pr 8, 1.0e7,1.0e7,1.0e9, 1,4.4875,0, 0,0
pr 9, 1.0e7,1.0e7,1.0e9, 1,5.8000,0, 0,0
pr 10, 1.0e7,1.0e7,1.0e9, 1,0.0000,0, 0,0
*
* MAIN9 solution data
*
sc 25000,1,0,1, 1.0e-6,1000,0, 0.00001,0,1.4, 1.0
ic 1,1505,2,0,527.5
mo 1,1101,2
mo 4,3001,1
, 4,3002,1
, 4,3003,1
, 4,3004,1
, 4,3005,1
, 4,3006,1
, 4,3007,1
*
end

```

2.12.9.2 Appendix B – Libra Static Impact Analysis Input File

```
ti static impact analysis
*
mc 23
*option list_input
option lh_check
*
lc 1,1, 0,0,0, 0,1,0, 0,0,1 ; head-on drop
lc 2,2, 0,0,0, 1,0,0, 0,0,1
*
skip
cnd 1, 23.3,-8,0
, 2, 37.5,-8,0
, 3, 37.5,27.9,0
, 4, 23.3,13.3,0
, 5, 20.1,16.5,0
, 6, 25.6,33.4,0
, 7, 13.3,36.7,0
, 8, 13.3,29.125,0
, 9, 3.0,16.5,0
, 10, 3.0,29.125,0
, 11, 19.4,35.3,0
, 12, 31.7,30.9,0
, 13, 13.3,16.5,0
*
* generate first meridian
*
g10
9,9, 1,1, 8,1, 0,1
1,2,3,4
-1
*
g10
9,5
4,3,6,5
6, 12
-1
*
g10
9,5
5,6,7,13
6, 11
-1
*
g10
5,6
9,13,8,10
-1
*
* merge nodes
*
me 0.05
end
```

```

skip
*
* generate 3d region
*
g32
    15,180, 1000,0
*
* center section
*
nd 101001, 0,16.5,0, 6, 0,2.525,0
el 101001,20,1,101001, 172, 1172,101002, 177, 1177,5,1,5,5,1,5,5
el 101011,20,1,101001, 1172, 2172,101002, 1177, 2177,5,1,5,5,1,5,5
el 101021,20,1,101001, 2172, 3172,101002, 2177, 3177,5,1,5,5,1,5,5
el 101031,20,1,101001, 3172, 4172,101002, 3177, 4177,5,1,5,5,1,5,5
el 101041,20,1,101001, 4172, 5172,101002, 4177, 5177,5,1,5,5,1,5,5
el 101051,20,1,101001, 5172, 6172,101002, 5177, 6177,5,1,5,5,1,5,5
el 101061,20,1,101001, 6172, 7172,101002, 6177, 7177,5,1,5,5,1,5,5
el 101071,20,1,101001, 7172, 8172,101002, 7177, 8177,5,1,5,5,1,5,5
el 101081,20,1,101001, 8172, 9172,101002, 8177, 9177,5,1,5,5,1,5,5
el 101091,20,1,101001, 9172,10172,101002, 9177,10177,5,1,5,5,1,5,5
el 101101,20,1,101001,10172,11172,101002,10177,11177,5,1,5,5,1,5,5
el 101111,20,1,101001,11172,12172,101002,11177,12177,5,1,5,5,1,5,5
el 101121,20,1,101001,12172,13172,101002,12177,13177,5,1,5,5,1,5,5
el 101131,20,1,101001,13172,14172,101002,13177,14177,5,1,5,5,1,5,5
el 101141,20,1,101001,14172,15172,101002,14177,15177,5,1,5,5,1,5,5
*
cs 0
*
* inside foam bc
*
bc 101001,1,1, 2,0
bc 1,16,1000, 13,0
, 10,16,1000, 13,0
, 19,16,1000, 13,0
, 28,16,1000, 13,0
, 37,16,1000, 13,0
, 46,16,1000, 13,0
, 55,16,1000, 13,0
, 64,16,1000, 123,0
, 73,16,1000, 123,0
, 91,16,1000, 123,0
, 100,16,1000, 123,0
, 109,16,1000, 123,0
, 118,16,1000, 123,0
, 136,16,1000, 2,0
, 145,16,1000, 2,0
, 154,16,1000, 2,0
, 163,16,1000, 2,0
, 176,16,1000, 2,0
, 175,16,1000, 2,0
, 174,16,1000, 2,0
, 173,16,1000, 2,0
, 172,16,1000, 2,0
*

```

```

* symmetry bc
*
nd 100001, -50, -8,0
, 100002, 50, -8,0
, 100003, 0, 50,0
*locate_bc 100001,100002,100003, 0.1,3,0, 0
*
me 0.05
*
* properties
*
* 20 lb foam @ 70 deg F
pr 1, 101
, 101, 0.3, .1,1890, .2,1915, .3,1940, .4,2168, 102
, 102, .5,2604, .6,3561, .65,4858, .7,5397
*
* bi-linear foam stress-strain properties
*pr 1, 101
, 101, 0.3, .1,1900, .2,2440, .3,2980, .4,3520, 102
, 102, .5,4060, .6,4600, .65,4870, .7,5140
*
pr 201,202,0.125
, 28.0E6,0.3,1.0E-5,0.000776, 1.0E6,40.0E3
*
* MAIN23 solution data
*
SC 700,0,0.01, 0.002,1,50, 0,1,8.0e6
*
end

```

2.12.9.3 Additional Information (December 1, 2011)

2.12.9.3.1 Contact Elements in Foam-Cask Model

The two input files used to develop the presentation in Appendix 2.12.9 are:

- foam-cask.t5
- head-on-drop.t5

The foam-drop.t5 input file is a dynamic analysis, while the head-on-drop.t5 input file is a static analysis similar to the analyses used in the SAR. In many LIBRA analyses, the input file type is designated as t5. This is a throw-back to when input data was on TAPE 5.

In the dynamic analysis, foam-cask.t5, both the foam-ground and foam-cask contacts are modeled by STIF1 elements. The LIBRA STIF1 elements can model gapped, contact interfaces, as described in the LIBRA help file for STIF1, listed below.

Figure 2-79 is an illustration of the foam-cask.t5 Libra model, and shows the application of STIF1 elements as gapped interfaces. In Figure 2-79 the blue region is the foam, and the green region is the cask. STIF1 gap elements 3001 through 3007 model the interface between the ground and foam, while elements 2001 through 2012 model the interface between the foam and cask. In the dynamic analysis, both foam and cask are assigned an initial velocity corresponding to a 30-ft. free fall, and impact forces are based upon gap closures.

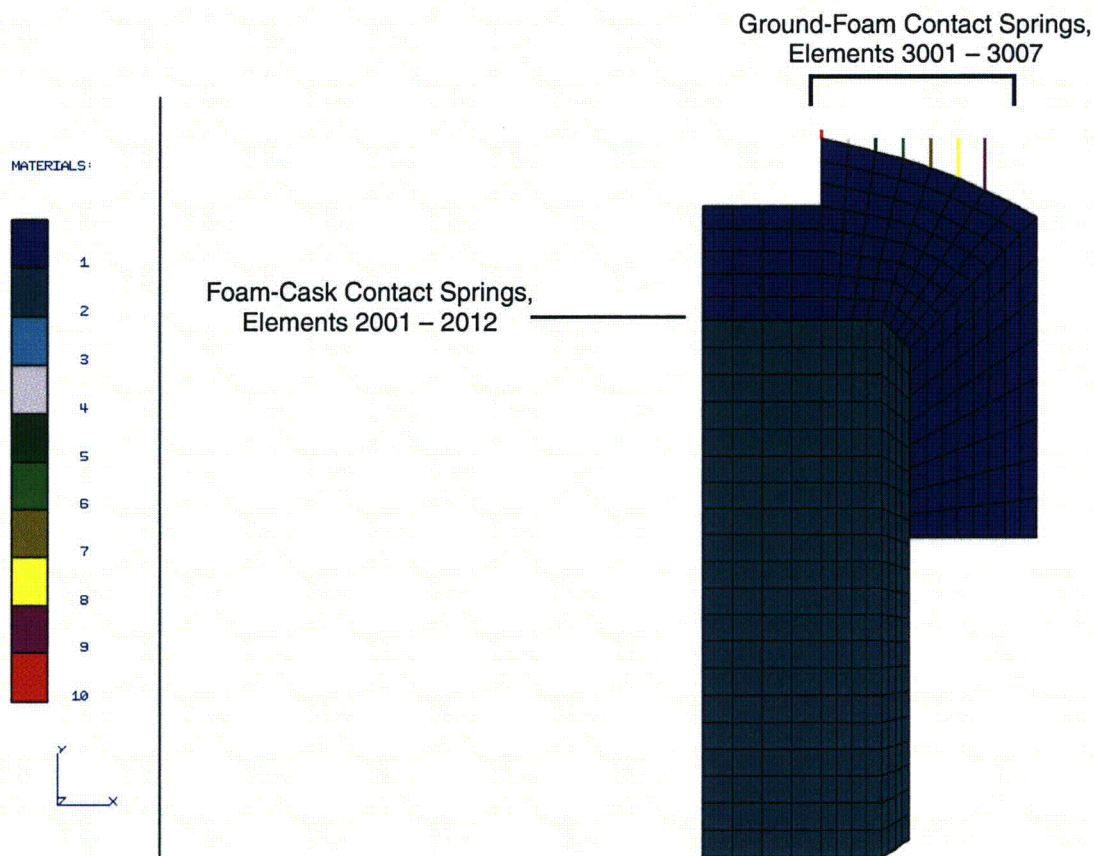


Figure 2-79. foam-cask.t5 LIBRA Model

2.12.9.3.2 Spring/Gap Element (STIF1)

STIF1 is a single degree of freedom spring element. The element is oriented by the two element nodes, or by a specified local coordinate system. The element can be applied in elastic, and elasto-plastic problems. This element can be used in both 2D and 3D problems.

STIF1 can be used to specify compression- or tension-only gaps in MAIN2 and MAIN9 analyses. If used as a gap element, the plasticity flag must be set on the Solution Control record. A single element cannot be modeled as both gapped and elasto-plastic.

If STIF1 is used as a gap element, LIBRA uses the penalty method to model the gap. As a result, it is important to enter a reasonably accurate value for the elastic stiffness; otherwise, the solution can be inaccurate. One method for determining nodal stiffness values is to apply unit loads in linear, static analyses.

2.12.9.3.2.1 STIF1 Element Property Record

Table 2-338. STIF1 Element Property Record

| Item | Description | Symbol |
|------|---|----------------|
| | Descriptor (PR) | |
| | Property set number | NM |
| 1 | Elastic stiffness | K |
| 2 | Inelastic stiffness | K1 |
| 3 | Spring yield force | F _y |
| 4 | Flag for gap/compression only effects ^{a, b} | IGAP |
| 5 | Initial gap value ^c | GAP |
| 6 | Local coordinate system for orienting spring ^d | NLCS |
| 7 | Dummy entry | (0) |
| 8 | Set initial gap to element length ^e | LGAP |

a. Set IGAP = 1 for a compression-only gap; set IGAP=2 for a tension-only gap; otherwise, for ordinary spring, set IGAP = 0.

b. Gap elements are considered to be elastic; however, dummy values must be entered for K1 and F_y, to maintain their data position.

c. GAP is entered as a positive value. For element nodal displacements U1 and U2, gaps are closed when the following is true:

$$\text{Compression (IGAP = 1)} \quad U2-U1 < -GAP$$

$$\text{Tension (IGAP = 2)} \quad U2-U1 > GAP$$

d. By default, the spring and gap are oriented by the two element nodes. To specify the spring and gap orientation, set NLCS to the number of a local coordinate (LC) system that defines the orientation. The spring is then oriented along the NLCS x-axis, and the gap is measured along the NLCS x-axis, with a positive gap in the +x direction.

e. If LGAP = 1, the initial gap size is set to the element length.

2.12.9.3.2.2 STIF1 Stress Output

Post processing data components for both elastic and inelastic problems are spring load (P) and spring deflection (d).

2.12.10 Effect of Ribs on Stress at Foam-Cask Interface

The effect of ribs inside the foam at the cask-cask lid interface is analyzed by the FEA model shown in Figure 2-80 and Figure 2-81. This model represents a section of foam impact limiter, steel cask, and steel rib, simplified by removing curvature. The section analyzed is a 10 × 10 × 10 in. foam block, positioned on a 5-in. section of the steel cask, and a steel rib embedded inside the foam block. The entire FEA model contains approximately 320,000 DOF, and is shown in Figure 2-80. The embedded rib is shown in the FEA model section in Figure 2-81. The nodal spacing throughout the model is 0.25 in. In the analysis, a uniform, 1-in., Z-displacement is applied to the top of the foam block, and the block is fixed in the Z-direction, at the base of the cask.

Figure 2-82 and Figure 2-83 display a central section of the cask model. Cask Z-displacement is shown in Figure 2-82, and cask Z-directional stress is shown in Figure 2-83. A central model section is selected to remove model edge effects. These two figures show that both displacement and stress perturbations due to the rib are localized to within an inch of the rib location. In accordance with Saint-Venant's Principle, these perturbations do not have a significant effect on cask stress.

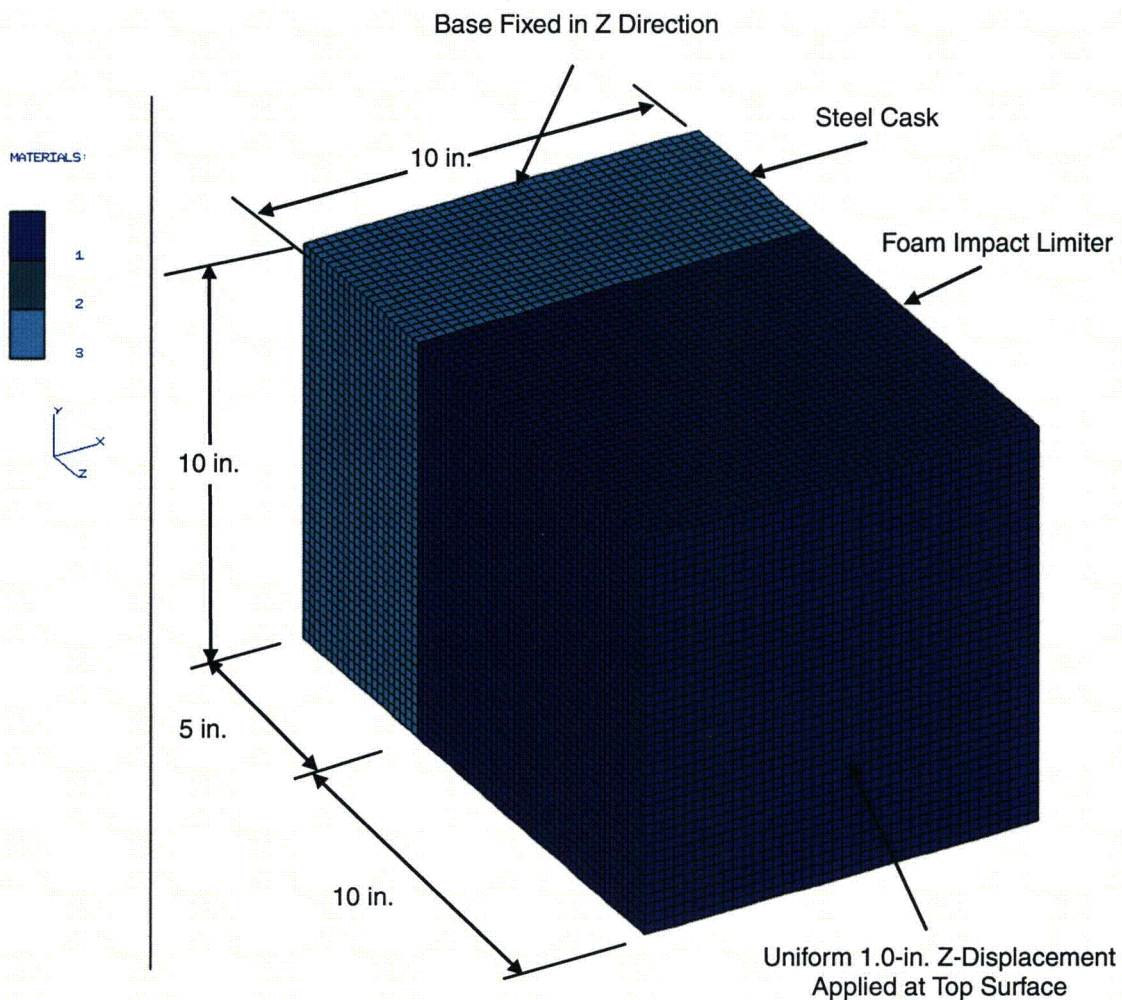


Figure 2-80. FEA Model Used in Rib Study

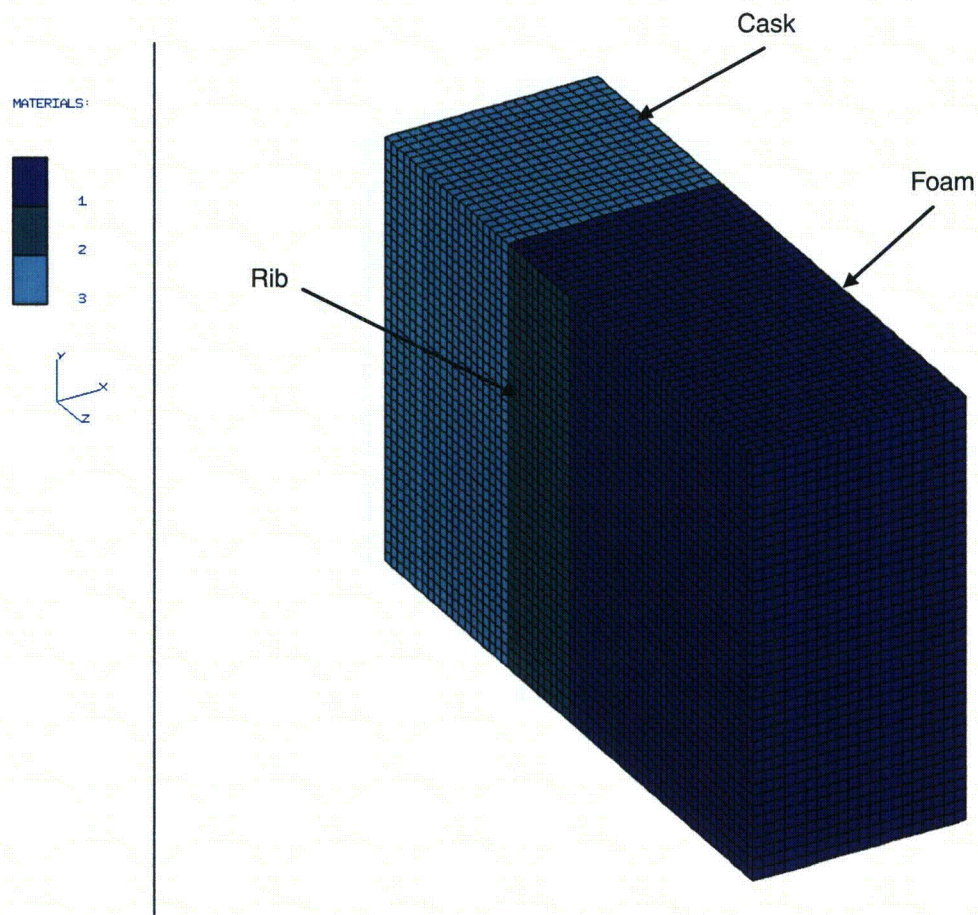


Figure 2-81. FEA Model Section Showing Rib

VECTOR: 1
 DOF: 3
 MIN: -6.5613E-03
 MAX: 0.0000E+00

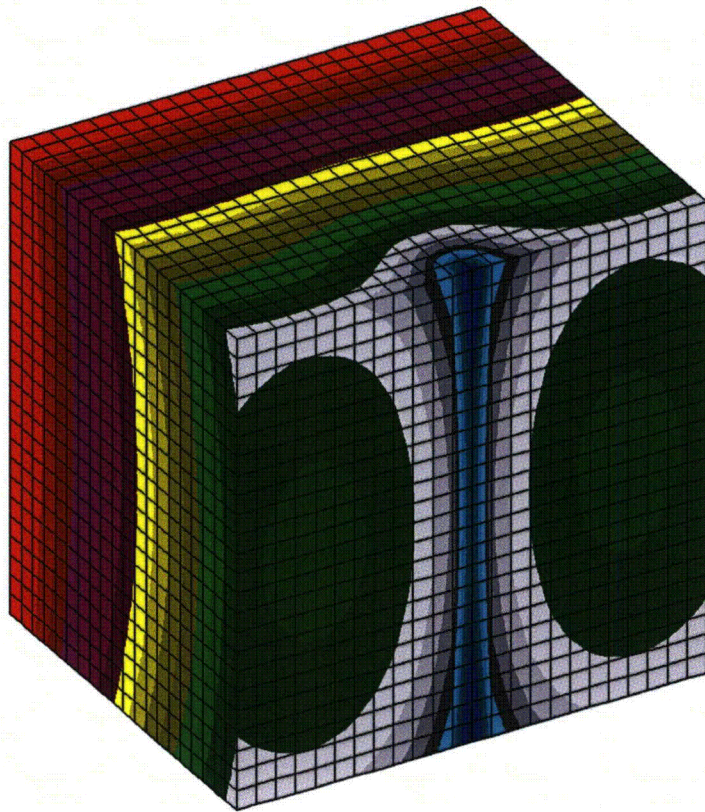
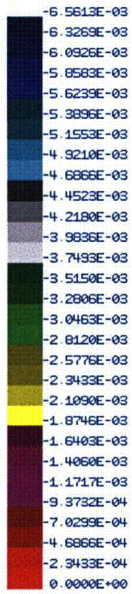


Figure 2-82. Z-Cask Section Z-Displacements

ELEM TYPE: 10
COMPONENT: 3
VECTOR: 1

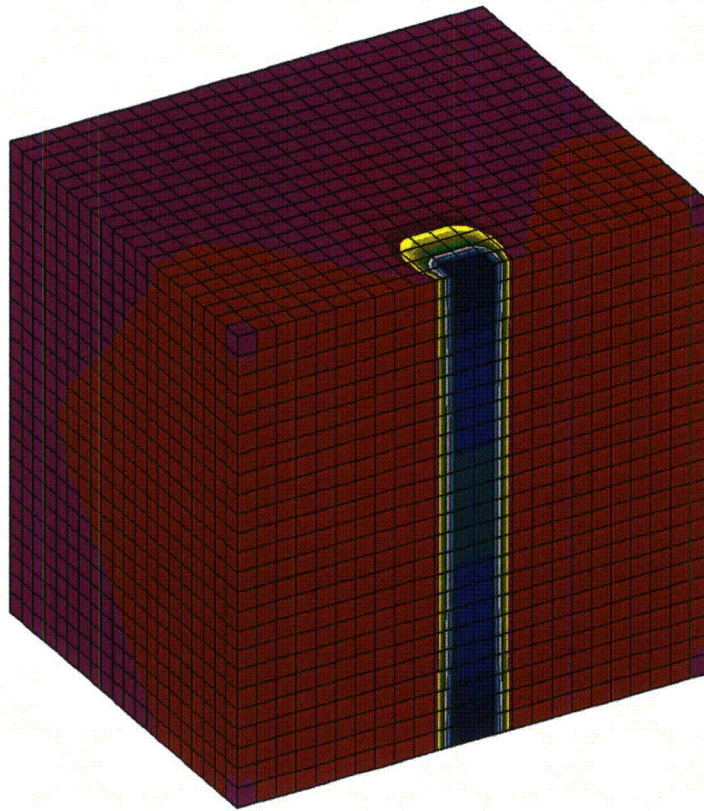
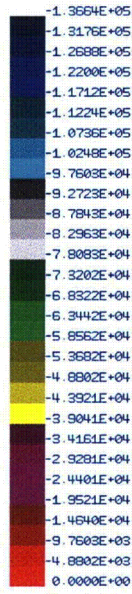


Figure 2-83. Cask Section Z-Stress

2.12.11 Analysis of 30-Ft. Drops with Shipping Cages

Shipping cages and pallets add to the cask impact forces for both Head-On and Cg/Corner 30-ft. Drops. In 30-ft. Side Drops, the shipping cage wire mesh panels impact the cask with negligible force. For Head-On and Cg/Corner Drops, the pallet impacts the cask through the upper impact limiter. As illustrated in Figure 2-84, the pallet impacts the upper impact limiter, while cask impacts the lower impact limiter.

The ground force reacts to both the pallet and cask inertia forces, as illustrated in Figure 2-84. In this analysis, the increase in the ground reaction force due to the pallet impact is evaluated. The upper and lower impact limiters exhibit different stiffness and frequency properties due to the difference in cask and pallet mass. As a result, the pallet inertia force and ground reaction force are not in phase. Dynamic analyses are required to account for the phase difference in the pallet and cask forces, so LIBRA-AGS analyses are performed for the 30-ft drops.

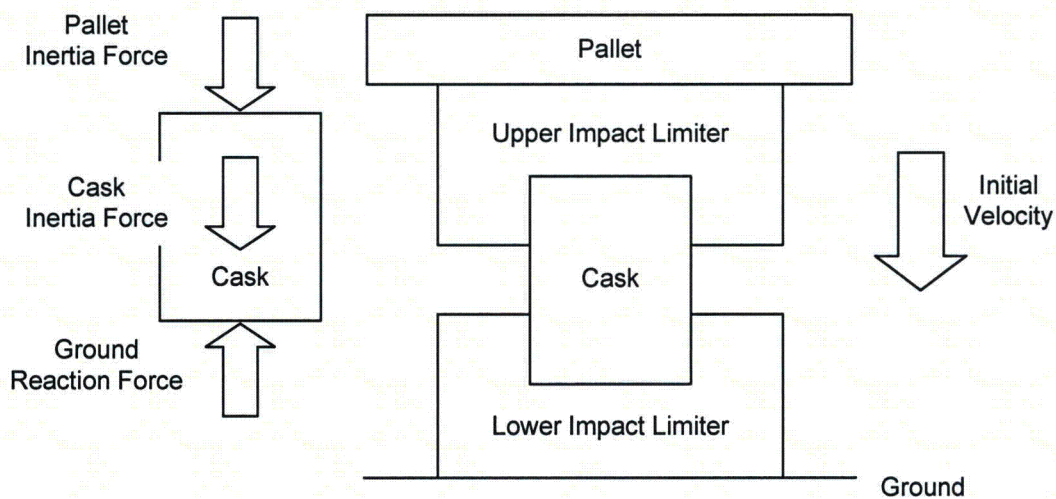


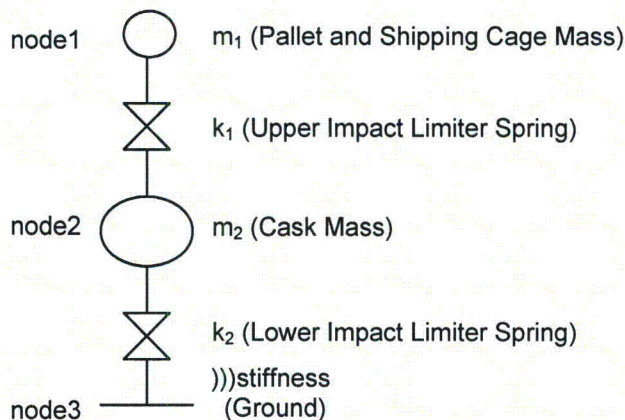
Figure 2-84. Configuration of Cask and Pallet Impact

Note: Figure 2-84 shows the scenario that the analysis evaluates. In this case, it is required that the assembled package be upside down.

2.12.11.1 Description of AGS Analyses

The LIBRA-AGS program is applied to the analyses of 30-ft. cask drops that include shipping cage impacts. The generalized dynamic model illustrated in Figure 2-85 is used for all drop analyses. The model contains two masses representing the pallet and cask, and two piecewise linear springs representing the upper and lower impact limiters. Spring stiffness values are taken from the impact limiter, load-displacement curves for 30-ft. drop analyses. A 30-ft. free-fall velocity is applied to both pallet and cask mass, as initial conditions. For each transport package model and each drop configuration, analyses are performed with, and without, the pallet mass. The effect of the pallet is measured by the difference in the ground impact force with, and without, the pallet mass.

AGS models for the Model AOS-025, AOS-050, and AOS-100 cask configurations differ only in nodal mass and element stiffness values, and AGS models for Head-On and Cg/Corner Drop analyses differ only in spring stiffness. A typical AGS input file is listed in Figure 2-85. The generalized stiffness and mass properties used in the analyses are presented in Table 2-339 and Table 2-340. Additionally, Table 2-339 lists the spring stiffness properties developed from the impact limiter load-displacement analyses. For Head-On Drop analyses, the generalized spring stiffness is modeled as bilinear. For Cg/Corner Drops, the generalized spring stiffness is modeled as trilinear.



```

ti  model 100 + pallet cg/corner drop
sc  10000,5.0e-6, 0.0,0.000, 3,0, 1
nd  1,3.88e-6
,   2,28.5
,   3,1.0
el  1,1, 1,2
,   2,1, 2,3
pr  1, 5.2e4,2.6e5, 8.6e4,6.0e5, 2.4e5,1.0e9
bc  3
iv  1,527.5
,   2,527.5
mo  1,1
,   2,1
,   1,4
,   2,4
end

```

Figure 2-85. AGS Model and Typical Input File

In Table 2-339, the first column lists the transport package model number and drop orientation. The generalized stiffness values are determined from the SAR figures listed in column 2. k_1 , k_2 , and k_3 are piecewise stiffness values. P_1 , P_2 , and P_3 are associated terminal force values. Figure 2-86 and Figure 2-87 are force-displacement plots that illustrate piecewise linear stiffness representations for the Model AOS-100. Piecewise linear stiffness representations for the Model AOS-025 and AOS-050 are similar. Table 2-340 lists the generalized pallet and cask mass values, m_1 and m_2 . Both the pallet and shipping cage mass are included in the m_1 values.

Table 2-339. Generalized Stiffness Properties – All Models

| Model and Drop Orientation | Reference Figure | k_1 (lb/in) | P_1 (lb) | k_2 (lb/in) | P_2 (lb) | k_3 (lb/in) | P_3 (lb) |
|----------------------------|------------------|------------------|---------------|------------------|---------------|------------------|---------------|
| AOS-025, Head-On | Figure 2-54 | 1.00E+05 | 6.00E+04 | 1.71E+05 | 1.00E+09 | – | – |
| AOS-025 Cg/Corner | Figure 2-56 | 3.56E+04 | 4.00E+04 | 6.40E+04 | 8.00E+04 | 1.60E+05 | 1.00E+09 |
| AOS-050 Head-On | Figure 2-57 | 8.88E+04 | 2.00E+05 | 1.37E+05 | 1.00E+09 | – | – |
| AOS-050 Cg/Corner | Figure 2-59 | 2.91E+04 | 8.00E+04 | 5.00E+04 | 1.80E+05 | 8.22E+04 | 1.00E+09 |
| AOS-100 Head-On | Figure 2-60 | 1.70E+05 | 5.00E+04 | 3.10E+05 | 1.00E+09 | – | – |
| AOS-100 Cg/Corner | Figure 2-63 | 5.20E+04 | 2.60E+05 | 8.60E+04 | 6.00E+05 | 2.40E+05 | 1.00E+09 |

Table 2-340. Generalized Pallet and Cask Mass Properties – All Models

| Model | m_1 (lb-sec ² /in) | m_2 (lb-sec ² /in) |
|---------|------------------------------------|------------------------------------|
| AOS-025 | 0.142 | 0.505 |
| AOS-050 | 0.621 | 3.26 |
| AOS-100 | 3.88 | 28.5 |

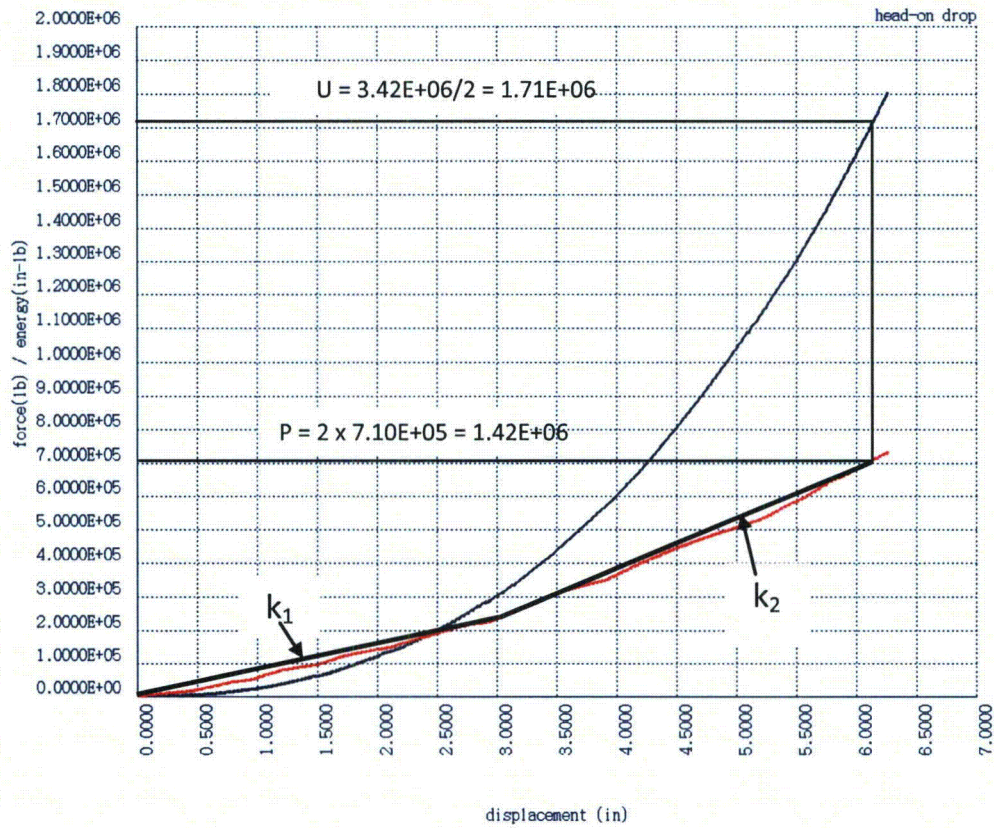


Figure 2-86. Bilinear Representation of Head-On Force-Displacement – Model AOS-100

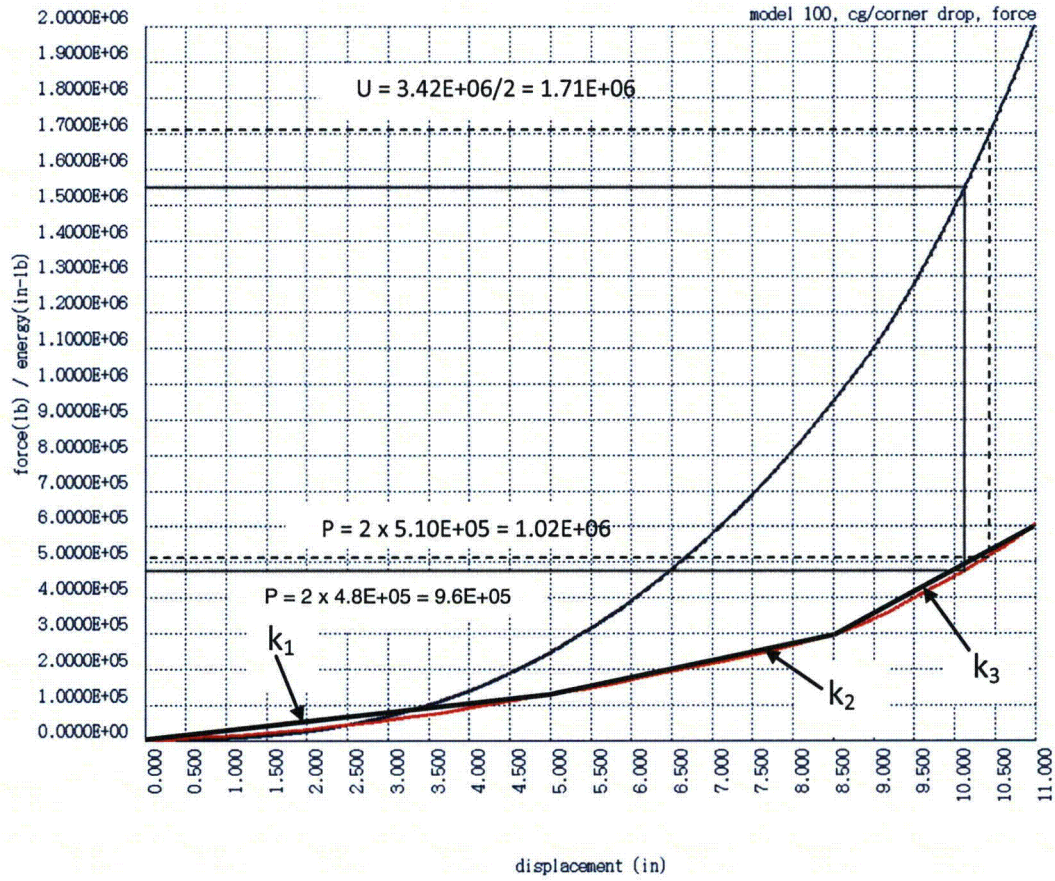


Figure 2-87. Trilinear Representation of Cg/Corner Force-Displacement – Model AOS-100

2.12.11.2 Results of AGS Analyses

Results of analyses for the Model AOS-100 are presented in Table 2-340, and Figure 2-88 and Figure 2-89. Figure 2-88 illustrates time-history plots of pallet mass displacement (1), and cask mass displacement (2). Figure 2-89 illustrates time-history plots of upper impact limiter spring force (3), and lower impact limiter spring force (4).

Table 2-341, Table 2-342, and Table 2-343 present results of analyses for Models AOS-025, AOS-050, and AOS-100, respectively. Each table lists maximum nodal displacements and maximum element forces. Definitions of column data for all three tables are listed after Table 2-341. Each model and drop configuration is analyzed with, and without, the pallet mass. Analyses including pallet mass are designated with "+ Pallet" (for example, "Head-On + Pallet"). Forces and displacements determined in the SAR static impact limiter analysis are included for comparison, in columns labeled F_s and δ_s .

Table 2-344 presents the change in ground impact forces due to the pallets. The F_s column lists the impact forces determined in the impact limiter static drop analyses. The ΔF column lists the increase in dynamic impact force due to the pallet. Values for ΔF are differences in P_2 force for impacts with, and without, the pallet. Using the information presented in Table 2-341, Table 2-342, and Table 2-343, ΔF is the difference between rows 1 and 2 for Head-On Drops, and rows 3 and 4 for Cg/Corner Drops. The F_T column lists the sum of F_s and ΔF . The Ratio column lists the F_T / F_s values, and measures the change in ground impact force due to pallet impact.

Table 2-341. AGS Analysis – Model AOS-025

| Drop | δ_1 (in.) | δ_2 (in.) | F_1 (lbs.) | F_2 (lbs.) | δ_s (in.) | F_s (lbs.) | Ratio |
|--------------------|---------------------|---------------------|-----------------|-----------------|---------------------|-----------------|-------|
| Head-On | – | 1.09 | – | 1.46E+05 | 1.10 | 1.40E+05 | – |
| Head-On + Pallet | 1.35 | 1.09 | 0.30E+05 | 1.44E+05 | – | – | 1.06 |
| Cg/Corner | – | 1.86 | – | 9.84E+04 | 1.90 | 10.0E+04 | – |
| Cg/Corner + Pallet | 2.77 | 1.93 | 3.80E+04 | 10.9E+04 | – | – | 1.11 |

where:

- δ_1 = Pallet deflection
- δ_2 = Cask deflection
- F_1 = Upper impact limiter spring force
- F_2 = Lower impact limiter spring force
- δ_s = Foam static analysis displacement
- F_s = Foam static analysis force
- Ratio = Ratio of P_2 with pallet to P_2 without pallet

Table 2-342. AGS Analysis – Model AOS-050

| Drop | δ_1 (in.) | δ_2 (in.) | F_1 (lbs.) | F_2 (lbs.) | δ_s (in.) | F_s (lbs.) | Ratio |
|--------------------|---------------------|---------------------|-----------------|-----------------|---------------------|-----------------|-------|
| Head-On | – | 3.13 | – | 3.20E+05 | 3.25 | 3.40E+05 | – |
| Head-On + Pallet | 4.19 | 3.28 | 8.55E+04 | 3.40E+05 | – | – | 1.06 |
| Cg/Corner | – | 5.18 | – | 2.15E+05 | 5.30 | 2.40E+05 | – |
| Cg/Corner + Pallet | 7.12 | 5.36 | 5.91E+04 | 2.30E+05 | – | – | 1.07 |

Table 2-343. AGS Analysis – Model AOS-100

| Drop | δ_1 (in.) | δ_2 (in.) | F_1 (lbs.) | F_2 (lbs.) | δ_s (in.) | F_s (lbs.) | Ratio |
|--------------------|---------------------|---------------------|-----------------|-----------------|---------------------|-----------------|-------|
| Head-On | – | 6.17 | – | 1.50E+06 | 6.10 | 1.42E+06 | – |
| Head-On + Pallet | 8.03 | 6.37 | 3.00E+05 | 1.56E+06 | – | – | 1.04 |
| Cg/Corner | – | 10.9 | – | 1.07E+06 | 10.5 | 1.02E+06 | – |
| Cg/Corner + Pallet | 14.4 | 11.1 | 2.09E+05 | 1.12E+06 | – | – | 1.05 |

Table 2-344. Increased Ground Impact Forces – All Models

| Model | Drop Orientation | F_s (lbs.) | ΔF (lbs.) | F_T ($F_s + \Delta F$) (lbs.) | Ratio (F_T/F_s) |
|---------|------------------|-----------------|----------------------|---|------------------------|
| AOS-025 | Head-On | 1.44E+05 | 0.80E+04 | 1.52E+05 | 1.06 |
| | Cg/Corner | 1.00E+05 | 1.06E+04 | 1.11E+05 | 1.11 |
| AOS-050 | Head-On | 3.40E+05 | 2.00E+04 | 3.60E+05 | 1.06 |
| | Cg/Corner | 2.40E+05 | 1.50E+04 | 2.55E+05 | 1.06 |
| AOS-100 | Head-On | 1.42E+06 | 6.00E+04 | 1.48E+06 | 1.04 |
| | Cg/Corner | 1.02E+06 | 5.00E+04 | 1.07E+06 | 1.05 |

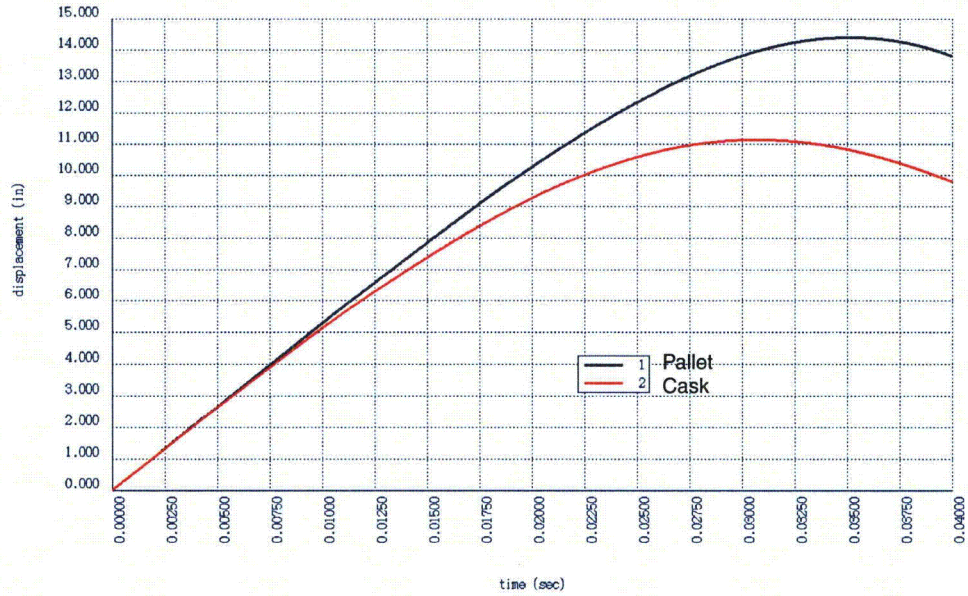


Figure 2-88. Model AOS-100 Cg/Corner Pallet and Cask Displacements

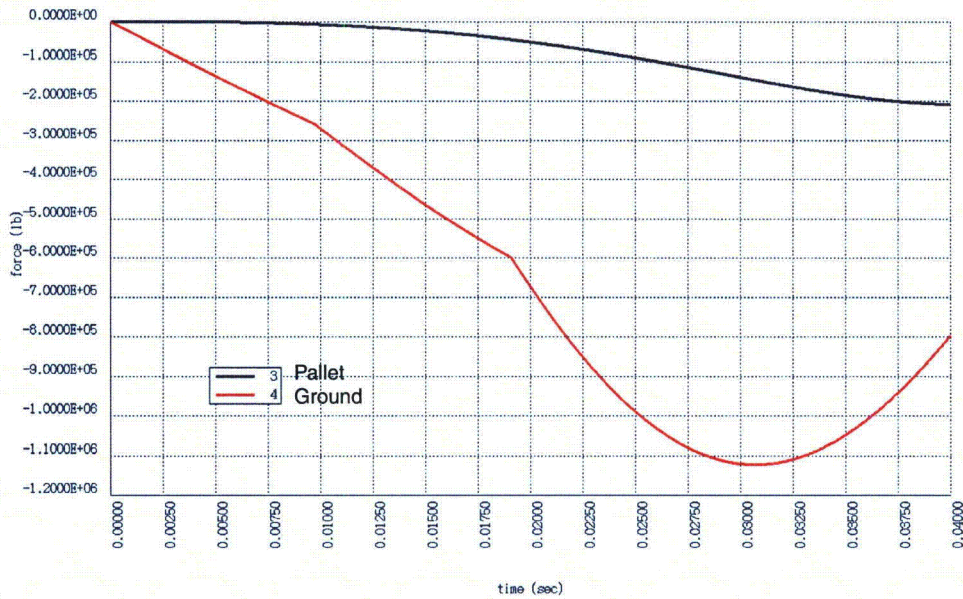


Figure 2-89. Model AOS-100 Cg/Corner Pallet and Ground Impact Forces

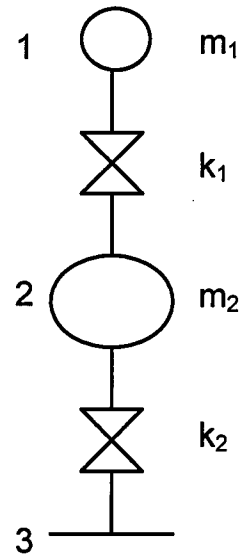
2.12.11.3 AGS Input Data for Cask and Pallet 30-Ft. Drop Analyses

```

ti    cask and pallet drop
*
sc    50000,5.0e-7, 0.0,0.000, 3,0, 0
*
*    model 100
*nd   1,3.88
*nd   2,28.5
*nd   3,1.0
*
*    model 050
nd    1,0.621
nd    2,3.26
nd    3,1.0
*
*    model 025
*nd   1,0.142e
*nd   2,0.505
*nd   3,1.0
*
el    1,1, 1,2
,     2,1, 2,3
*
*    100 head-on
*pr   1, 1.7e5,5.0e5, 3.1e5,1.0e9
*    100 cg/corner

*pr   1, 5.2e4,2.6e5, 8.6e4,6.0e5, 2.4e5,1.0e9
*
*    050 head-on
*pr   1, 8.88e4,2.00e5, 1.37e5,1.00e9
*    050 cg/corner
pr    1, 2.91e4,8.00e4, 5.00e4,1.80e5, 8.22e4,1.00e9
*
*    025 head-on
*pr   1, 1.00e5,6.00e4, 1.70e5,1.00e9
*    025 cg/corner
*pr   1, 3.56e4,4.00e4, 6.40e4,8.00e4, 1.60e5,1.0e9
*
bc    3
*
iv    1,527.5
,     2,527.5
*
mo    1,1
,     2,1
,     1,4
,     2,4
*
end

```



2.12.12 Analysis of Tie-Down Devices

2.12.12.1 Introduction

The Model AOS-050 and AOS-100 cask transport tie-down system is illustrated in Figure 2-90. The system consists of cables (four (4) in the Model AOS-050; eight (8) in the Model AOS-100), a shipping cradle under the lower LAST-A-FOAM FR-3700 series foam, and a tie-down ring over the upper LAST-A-FOAM FR-3700 series foam. The postulated inertia loading is 10g forward, 5g lateral, and 2g vertical. Lateral and vertical inertia forces are illustrated in Figure 2-90, as F and W, respectively. In Figure 2-90, the dimension H is the distance from the cask's center of gravity to lateral support.

The Model AOS-025 uses four tie-down straps.

Analyses are performed for 10g forward and 2g vertical inertia loads. Stress due to the 5g lateral load is interpolated from the 10g forward load analysis, because the tie-down configuration is axisymmetric. Stresses due to the three (3) inertia loads are combined where required, and compared to allowable stresses.

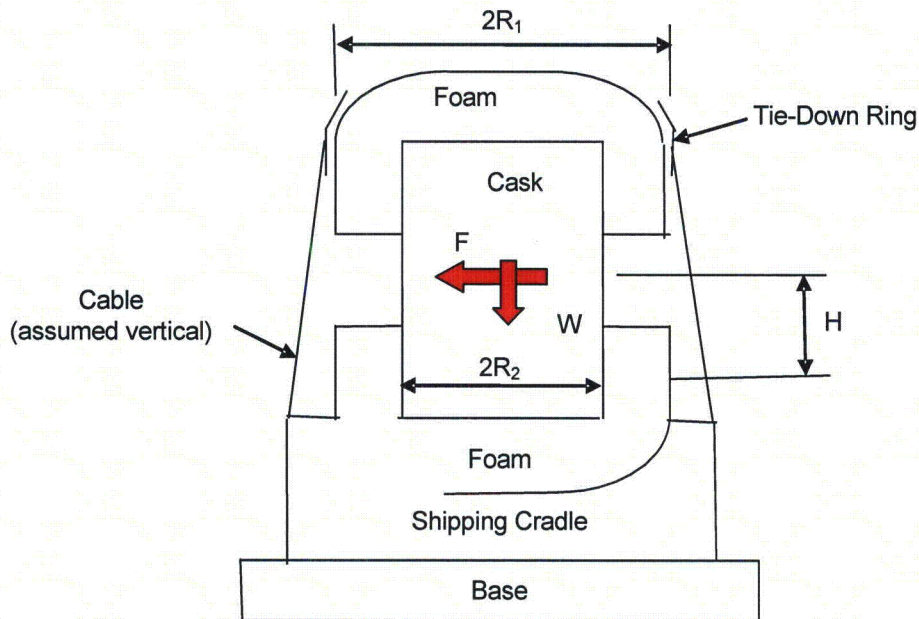


Figure 2-90. Tie-Down Schematic

2.12.12.2 Base Foam Vertical Bearing Force

The inertia force, F , illustrated in Figure 2-90 is assumed to produce the foam bearing traction illustrated in Figure 2-91, at the shipping cradle. The foam bearing traction is assumed sinusoidal in the circumferential direction, and linear in the horizontal direction, as illustrated in Figure 2-91. The bearing traction is provided by:

$$p = (p_0 / 2R_1) * (1 - \cos\theta) * r$$

where:

$$p_0 = \text{Maximum bearing traction}$$

The total bearing force is then:

$$\begin{aligned} P &= p_0 / 2R_1 \int_0^{2\pi} \int_{R_2}^{R_1} (1 - \cos\theta) * r^2 * dr * d\theta \\ &= \pi p_0 (R_1^3 - R_2^3) / 3R_1 \end{aligned}$$

The moment due to the bearing force is:

$$\begin{aligned} M &= p_0 / 2R_1 \int_0^{2\pi} \int_{R_2}^{R_1} (1 - \cos\theta)^2 * r^3 * dr * d\theta \\ &= 3\pi p_0 (R_1^4 - R_2^4) / 8R_1 \end{aligned}$$

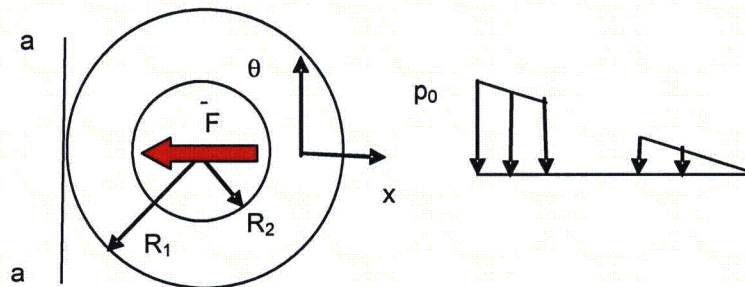


Figure 2-91. Bearing Traction Along Line $\theta = 0 - 180$

The overturning moment about the axis a-a in Figure 2-91 due to the inertia force is $F * H$:

$$F * H = (3\pi p_0 / 8R_1) * (R_1^4 - R_2^4)$$

Solving for maximum bearing traction:

$$p_0 = 8F * H * R_1 / (3\pi (R_1^4 - R_2^4))$$

Vertical foam bearing traction due to W is:

$$p_1 = W / [\pi (R_1^2 - R_2^2)]$$

2.12.12.3 Base Foam Lateral Bearing Force

The foam bearing force at the shipping cradle wall due to inertia force, F , is illustrated in Figure 2-92. The traction distributions are assumed to be sinusoidal in the circumferential direction. For vertical bearing length B , the total wall bearing force is:

$$F = 2B \int_0^{\pi/2} q * R_1 * \cos\theta * d\theta$$

Integrating:

$$F = 2B * R_1 * q$$

$$q = F / 2B * R_1$$

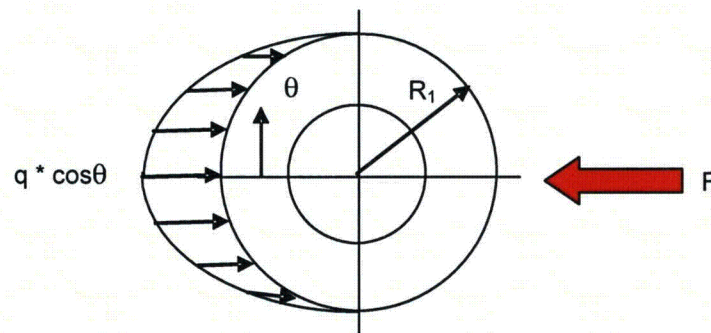


Figure 2-92. Schematic of Lateral Bearing Forces

2.12.12.4 Summary of Stress Equations for Base Foam

B = Lateral shipping cradle wall bearing length

F = Lateral inertia force

H = Lateral inertia force moment arm

R₁ = Outside foam radius

R₂ = Inside foam radius

T = Cable tension force

W = Vertical inertia force

1. Foam vertical traction due to inertial overturning moment:

$$p_0 = 8F * H * R_1 / 3\pi (R_1^4 - R_2^4)$$

2. Foam vertical traction due to vertical inertia:

$$p_1 = W / \pi (R_1^2 - R_2^2)$$

3. Foam horizontal traction due to lateral inertia:

$$q = F / 2B * R_1$$

2.12.12.5 Cable Force

The cable forces react the overturning moment due to the inertia force, F , and height, H , in Figure 2-90. Moment equilibrium is taken about axis a-a in Figure 2-93, with cable forces assumed proportional to the distance from axis a-a.

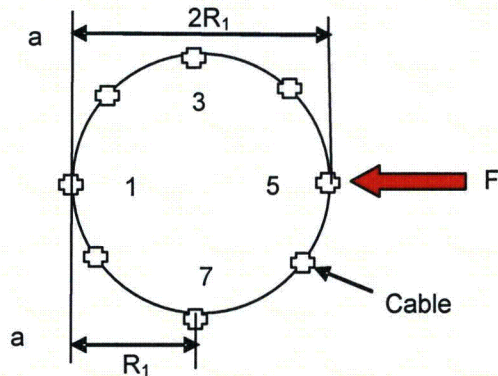


Figure 2-93. Tension Cables – Model AOS-100

Table 2-345. Model AOS-100 Cable Loads

| Cable | d | P/T | d * P/T | P (k) |
|----------|---------|---------|---------|--------|
| 1 | 0.00000 | 0.00000 | 0.00000 | 0.0000 |
| 2 | 6.73654 | 0.14645 | 0.98656 | 3.0560 |
| 3 | 23.0000 | 0.50000 | 11.5000 | 10.435 |
| 4 | 39.2635 | 0.85355 | 33.5134 | 17.813 |
| 5 | 46.0000 | 1.00000 | 46.0000 | 20.870 |
| 6 | 39.2635 | 0.85355 | 33.5134 | 17.813 |
| 7 | 23.0000 | 0.50000 | 11.5000 | 10.435 |
| 8 | 6.73654 | 0.14645 | 0.98656 | 3.0560 |
| Σ | - | 4.00000 | 138.000 | 83.478 |

where:

- d = Distance to axis a-a
- T = Maximum cable tension force
- P = Cable tension force, in kips (k)

From Figure 2-90:

$$M = F * H$$

$$F = 120 \text{ k}$$

$$H = 24 \text{ in.}$$

$$M = 120 * 24 = 2,880 \text{ in-k}$$

From Table 2-345, the maximum and total cable forces are:

$$M = \sum d * P / T$$

$$T = M / 138 = 2,880 / 138 = 20.870 \text{ k}$$

$$\sum P = 4.00 * 20.870 = 83.480 \text{ k}$$

2.12.12.6 Tie-Down Ring Foam Bearing Pressure

The tie-down ring is in equilibrium under the cable forces and foam bearing pressures, as illustrated in Figure 2-94. The bearing pressure due to the cable resultant forces is:

$$\begin{aligned} p &= P / A \\ P &= 83.478 \\ A &= \pi * (R_1^2 - R_2^2) = 857.7 \text{ in}^2 \\ p &= 0.0973 \text{ lb/in}^2 \end{aligned}$$

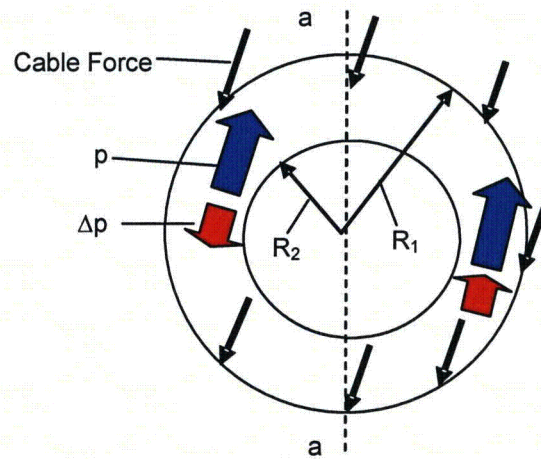


Figure 2-94. Bearing Pressure and Cable Forces

2.12.12.7 Tie-Down Ring Foam Differential Bearing Pressure

The moment about axis a-a in Figure 2-94 due to differential bearing pressure is:

$$\begin{aligned}M' &= 4 * \Delta p \int_0^{\pi/2} \int_{R_2}^{R_1} \cos\theta * r^2 * dr * d\theta \\ &= 4 / 3 * (R_1^3 - R_2^3) * \Delta p \\ \Delta p &= M' / [4 / 3 * (R_1^3 - R_2^3)]\end{aligned}$$

From Table 2-345, the moment about axis a-a in Figure 2-95 is:

$$\begin{aligned}M' &= M - (\Sigma P * R_1) \\ &= 2,880 - (83.480 * 23.0) \\ &= 961.34 \text{ in-k} \\ \Delta p &= 961.34 / 10,761 = 0.0893 \text{ lb/in}^2 \\ p + \Delta p &= 187.0 \text{ lb/in}^2 \\ p - \Delta p &= 8.000 \text{ lb/in}^2\end{aligned}$$

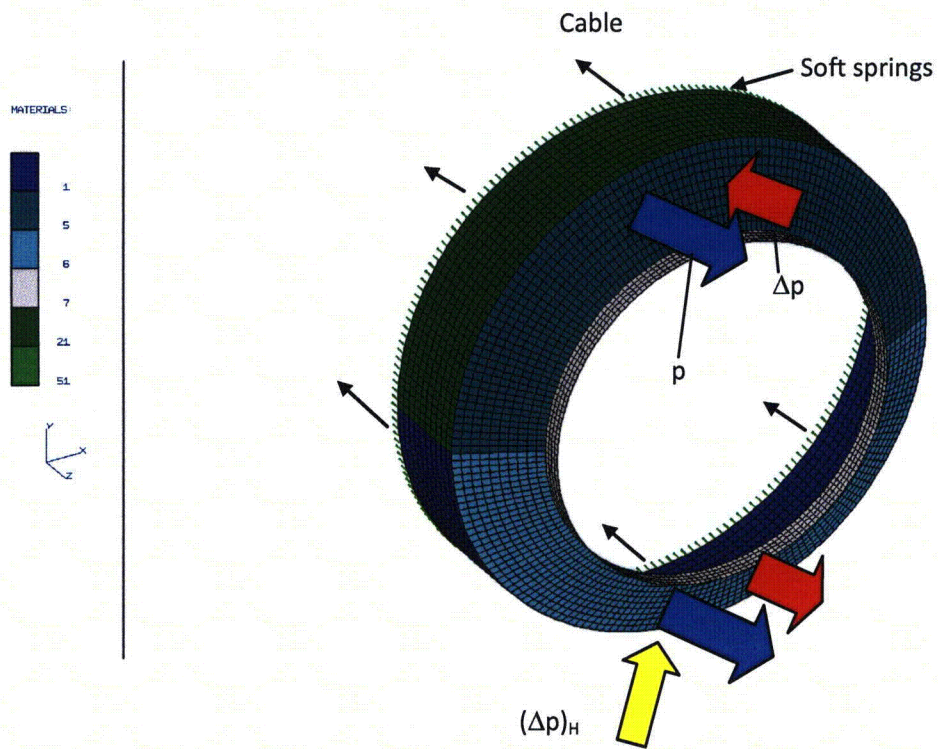


Figure 2-95. FEA Model of Tie-Down Ring

2.12.12.8 Horizontal Component of Differential Pressure

The Δp pressure acting on the conical shell produces a horizontal force resultant:

$$\begin{aligned} P_H &= 4 * \Delta p * \sin\alpha \int_0^{\pi/2} \int_{R_2}^{R_1} \cos\theta * r * dr * d\theta \\ &= 2 * \Delta p * \sin\alpha * (R_1^2 - R_2^2) \end{aligned}$$

where:

$$\alpha = \text{Conical shell base angle}$$

For radius, R_1 , and cylinder height, h :

$$P_H = P_H / 2R_1 * h$$

$$P_H = 2 * 89.3 * \sin 27.2^\circ = 2.23 \times 10^4 \text{ lbs.}$$

$$p_H = 2.23 \times 10^4 / 46.0 * 9.0 = 53.8 \text{ psi}$$

2.12.12.9 Analysis of Tie-Down Ring

The tie-down ring is analyzed for a 10g lateral inertia force by finite elements, using the FEA model illustrated in Figure 2-95. The ring is analyzed as a shell structure, and the FEA model contains 26,400 DOF, with 4,400 nodes and 4,300 quad shell elements. The model is composed of two primary sections – a cylindrical shell and a conical shell. A ring of soft springs is modeled about the base of the cylindrical section to react out-of equilibrium forces.

The loads applied to the model are illustrated in Figure 2-95. These loads are in equilibrium, and consist of the cable loads developed in Table 2-345, and bearing tractions on the conical and cylindrical shells. In Figure 2-95, the resultants of the bearing pressure, p , and differential bearing pressure, Δp , balance the cable force and cable moment resultants. The differential pressure, Δp , acting on the conical shell produces a horizontal force resultant, and this resultant is balanced by the pressure $(\Delta p)_H$ applied to the cylindrical shell.

Results of the tie-down ring stress analysis are presented in Figure 2-96 and Figure 2-97. Figure 2-96 illustrates lateral displacement of the conical shell, and Figure 2-97 illustrates the outer fiber maximum principal stress in the conical shell.

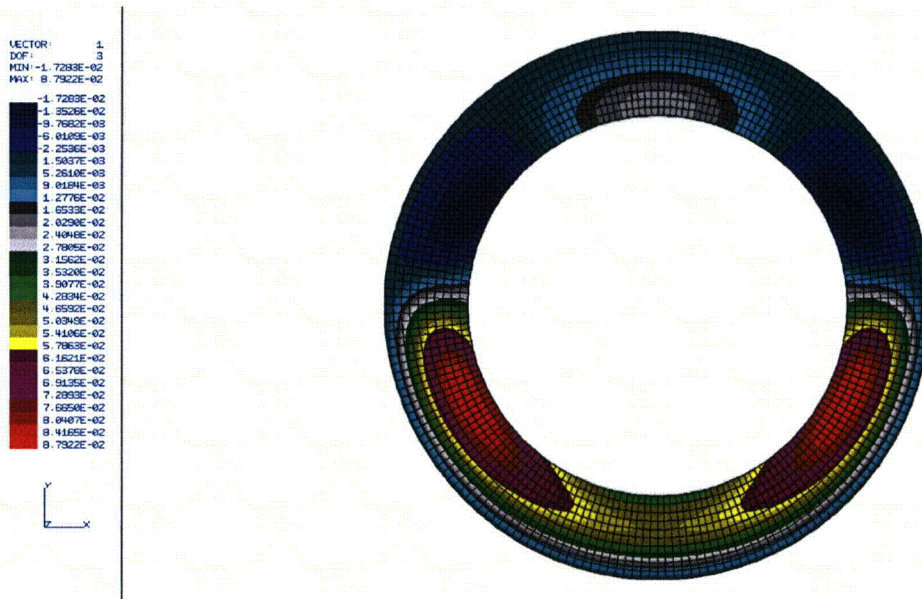


Figure 2-96. Lateral (Z) Displacement in Conical Shell – Model AOS-100

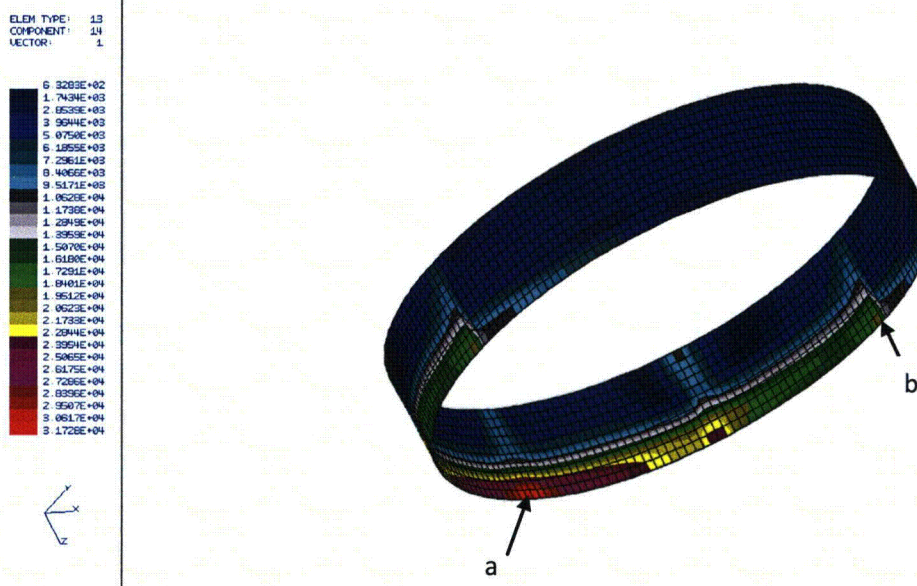


Figure 2-97. Maximum Principal Membrane Stress – Model AOS-100

2.12.12.10 Stress in Foam – Model AOS-100

The foam stress is limited to 10% strain to avoid excessive deformation. From the *Design Guide for Use of LAST-A-FOAM FR-3700 for Crash & Fire Protection of Radioactive Material Shipping Containers* (Reference [2.13]):

$$\begin{aligned}\sigma &= Y_{\text{int}} (\rho)^S \\ Y_{\text{int}} &= 4.3422 \\ \rho &= 12 \\ S &= 1.8809 \\ \sigma &= 4.3422 * 107.1 = 465.1 \text{ psi}\end{aligned}$$

Applying equations in Appendix 2.12.12.4:

$$\begin{aligned}B &= \text{Shipping cradle wall length} && 8.0 \text{ in.} \\ F &= \text{Lateral force} && 120,000.0 \text{ lbs.} \\ H &= \text{Cask center of gravity to shipping cradle} && 24.0 \text{ in.} \\ R_1 &= \text{Outside foam radius} && 23.0 \text{ in.} \\ R_2 &= \text{Inside foam radius} && 14.0 \text{ in.} \\ W &= \text{Vertical force} && 24,000.0 \text{ lbs.}\end{aligned}$$

Base foam vertical bearing stress (psi):

$$p = 8F * H * R_1 / 3\pi (R_1^4 - R_2^4) + W / \pi (R_1^2 - R_2^2) = 234 \text{ psi} (< 465.1)$$

Base foam lateral bearing stress (psi):

$$q = F / 2B * R_1 = 310 \text{ psi} (< 465.1)$$

From Appendix 2.12.12.7, the maximum foam bearing stress at the conical shell:

$$p + \Delta p = 187.0 \text{ psi} (< 465.1)$$

From Appendix 2.12.12.8, the maximum foam bearing stress at the cylindrical shell:

$$p_H = 107.7 \text{ psi} (< 465.1)$$

2.12.12.11 Stress in Tie-Down Ring – Model AOS-100

Figure 2-97 shows the maximum principal membrane stress for bending about the x-axis. The maximum stress occurs at location 'a', and is 31.7 ksi. For bending about the y-axis, the stress at location 'b' corresponds to the stress at location 'a'. The stress at location 'b' is 18.5 ksi for 10g loading. The combined stress due to 10g about the x-axis, and 5g about the y-axis, is then:

$$f = 32.2 + (1 / 2) * 18.5 = 41.5 \text{ ksi}$$

For AMS 4144F, aluminum alloy 2219T851, yield stress $F_y = 46.0$ ksi:

$$MS = 46.0 / 41.5 - 1.0 = 0.11$$

2.12.12.12 Stress in Cables – Model AOS-100

$P_1 =$ Maximum cable load (Table 2-345, cable 5) due to 10g forward inertia

$P_2 =$ Maximum cable load due to 5g lateral inertia

$P_3 =$ Cable load due to 1g vertical inertia

$$P_1 = 20.9 \text{ k}$$

$$P_2 = (1 / 2) * 20.9 = 10.5 \text{ k}$$

$$P_3 = 12 / 8 = 1.5 \text{ k}$$

$$P = P_1 + P_2 + P_3 = 32.9 \text{ k}$$

From *ASTM F1145 - 05(2011)*, Table 3 (Reference [2.27]), Jaw-Jaw, $P_u = 60$ k:

$$MS = 60 / 32.9 - 1.0 = 0.82$$

2.12.12.13 Forces – Model AOS-050

Note: Refer to Appendix 2.12.12.7 and Appendix 2.12.12.8 for further details.

Maximum cable tension, moment about axis a-a:

$$M = F * H = 2R_1 * (T / 2) + R_1 * 2T = 3R_1 * T$$

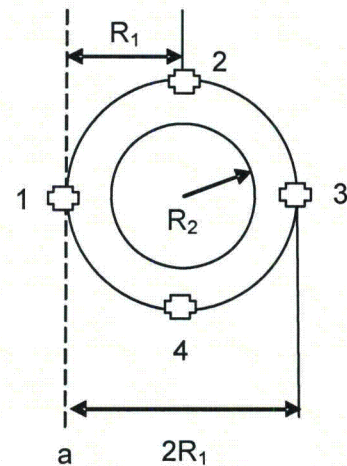
$$T = F * H / 3R_1$$

$$F = 11,810 \text{ lbs.}$$

$$H = 16 \text{ in.}$$

$$R_1 = 12 \text{ in.}$$

$$T = 5,248.9 \text{ lbs.}$$



Total force in cables:

$$P = T + 2 * T / 2 = 2T = 10,500 \text{ lbs.}$$

Conical shell bearing pressure:

$$p = P / A$$

$$P = 10,500$$

$$R_2 = 8.0$$

$$A = \pi * (R_1^2 - R_2^2) = 251.3 \text{ in}^2$$

$$p = 41.8 \text{ lb/in}^2$$

Differential conical shell bearing pressure:

$$M' = 4 / 3 * (R_1^3 - R_2^3) * \Delta p$$

$$= M - P * R_1 = 3R_1 * T - 2R_1 * T = R_1 * T$$

$$= 12 * 10,500 = 1.26 \times 10^5 \text{ in-lb}$$

$$\Delta p = M' / [4/3 * (R_1^3 - R_2^3)]$$

$$= 1.26 \times 10^5 / 1.621 \times 10^3 = 77.8 \text{ lb/in}^2$$

$$p + \Delta p = 119.6$$

$$p - \Delta p = -36.0$$

Pressure < 0, increase cable loads:

$$\begin{aligned}P' &= A * (p - \Delta p) = 251.3 * 36.0 = 9,046.7 \text{ lbs.} \\ \Delta T &= 9,046.7 / 4 = 2,261.7 \\ T(1) &= 0.0 + 2,261.7 = 2,261.7 \\ T(2) &= T(4) = 5,248.9 / 2 + 2,261.7 = 4,886.2 \text{ lbs.} \\ T(3) &= 5,248.9 + 2,261.7 = 7,510.6 \text{ lbs.} \\ p + \Delta p &= 119.6 + 36.0 = 155.6 \text{ psi} \\ p - \Delta p &= -36.0 + 36.0 = 0.0\end{aligned}$$

Horizontal component of differential pressure (refer to Appendix 2.12.12.8):

$$\begin{aligned}P_H &= 2 * \Delta p * \sin \alpha * (R_1^2 - R_2^2) \\ \alpha &= 27.2^\circ \\ P_H &= 2 * 77.8 * 0.4571 * (12^2 - 8^2) = 5,690.0 \text{ lbs.} \\ p_H &= P_H / 2R_1 * h = 5,690.0 / 24.0 * 4.5 = 52.6 \text{ psi}\end{aligned}$$

2.12.12.14 Stress in Cable – Model AOS-050

Maximum cable load from Appendix 2.12.12.13:

$$T = 7,510.6 \text{ lbs.}$$

From *ASTM F1145 - 05(2011)*, Table 3 (Reference [2.27]), Jaw-Jaw, $P_u = 60 \text{ k}$:

$$MS = 60 / 7.510 - 1 = 7.0$$

2.12.12.15 Stress in Foam – Model AOS-050

Allowable foam stress ($\epsilon = 0.1$):

$$\begin{aligned}\sigma &= Y_{\text{int}} (\rho)^S \\ Y_{\text{int}} &= 4.3422 \\ \rho &= 10 \\ S &= 1.8809 \\ \sigma &= 4.3422 * 76.0 = 330.1 \text{ psi}\end{aligned}$$

Applying equations in Appendix 2.12.12.4:

| | | | |
|----------------|---|---|---------------|
| B | = | Shipping cradle wall length | 4.0 in. |
| F | = | Lateral force | 11,810.0 lbs. |
| H | = | Cask center of gravity to shipping cradle | 16.0 in. |
| R ₁ | = | Outside foam radius | 12.0 in. |
| R ₂ | = | Inside foam radius | 7.0 in. |
| W | = | Vertical force | 2,362.0 lbs. |

Base foam vertical bearing stress (psi):

$$p = 8F * H * R_1 / 3\pi (R_1^4 - R_2^4) + W / \pi (R_1^2 - R_2^2) = 112.9 \text{ psi} (< 330.1)$$

Base foam lateral bearing stress (psi):

$$q = F / 2B * R_1 = 123.0 \text{ psi} (< 330.1)$$

From Appendix 2.12.12.12, the maximum foam bearing stress at the conical shell:

$$p + \Delta p = 155.6 \text{ psi} (< 330.1)$$

$$p_H = 52.6 \text{ psi} (< 330.1)$$

2.12.12.16 Stress in Tie-Down Ring – Model AOS-050

Figure 2-98 illustrates the maximum principal membrane stress for bending about the x-axis. The maximum stress occurs at location 'a', and is 13.5 ksi. For bending about the y-axis, the stress at location 'b' corresponds to the stress at location 'a'. The stress at location 'b' is 5.3 ksi for 10g loading. The combined stress due to 10g about the x-axis, and 5g about the y-axis, is then:

$$f = 13.5 + (1/2) * 5.3 = 16.2 \text{ ksi}$$

For ASME SB-209 Alloy 6061 T6, Yield Strength $F_y = 35.0$ ksi:

$$MS = 35.0 / 16.2 - 1.0 = 1.16$$

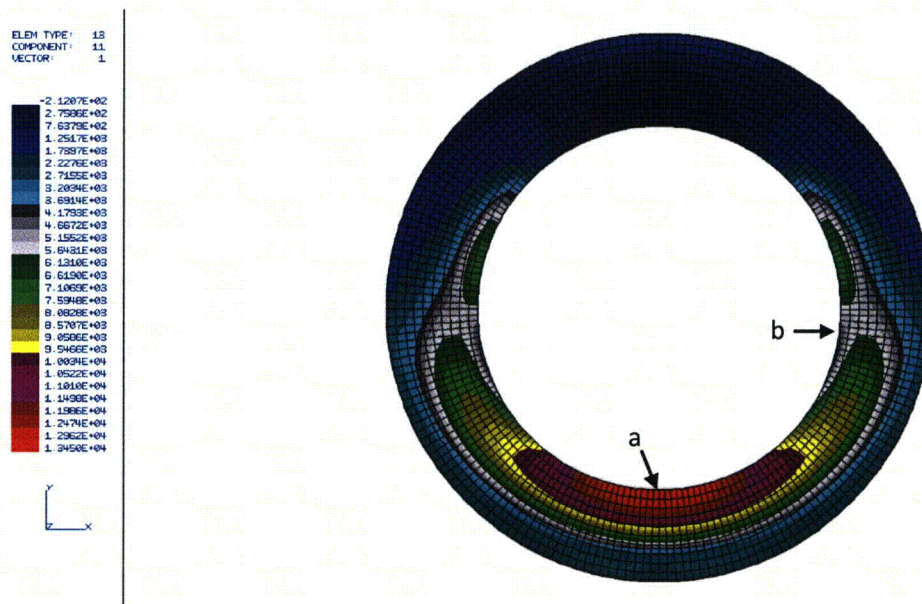


Figure 2-98. Maximum Principal Membrane Stress – Model AOS-050

2.12.12.17 Tie-Down Straps – Model AOS-025

Strap load:

$$\sum M_A = 0$$

$$11.8 * T_1 + 2T_1 / 2 * 5.9 = 1,680 * (16.25 - 2.30) / 2$$

$$T_1 = 1.172 \times 10^4 / 17.7 = 662.0 \text{ lbs.}$$

$$T_2 = T_1 / 2 = 331.0 \text{ lbs.}$$

$$T_3 = W / 4 = 42.0 \text{ lbs.}$$

$$T = T_1 + T_2 + T_3 = 1,035.0 \text{ lbs.}$$

For a 1.0-inch strap, $P_u = 3,000 \text{ lbs.}$:

$$MS = 3,000 / 1,035.0 - 1.0 = 1.90$$

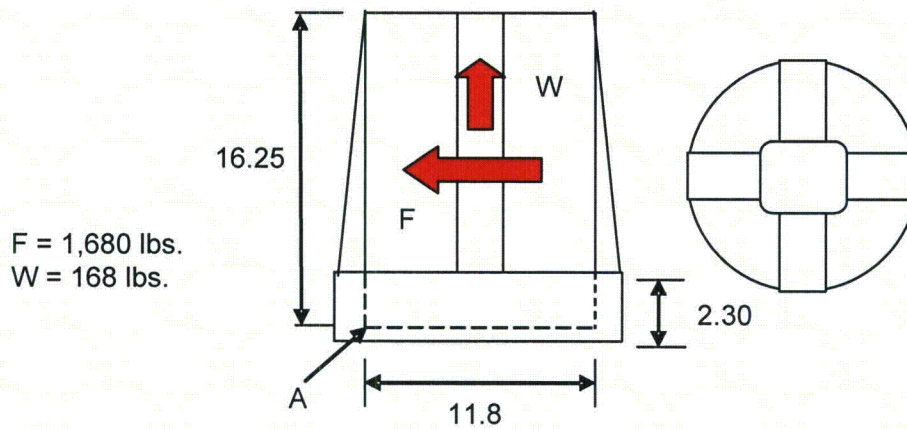


Figure 2-99. Tie-Down Strap Load – Model AOS-025

VECTOR: 1
 DOF: 3
 MIN: -2.0112E-03
 MAX: 1.4466E-02

| | |
|---|-----------|
| 2 | 0.112E-03 |
| 1 | 4.220E-03 |
| 8 | 3.266E-04 |
| 2 | 4.369E-04 |
| 3 | 4.164E-04 |
| 9 | 3.465E-04 |
| 1 | 5.239E-03 |
| 2 | 1.130E-03 |
| 2 | 7.622E-03 |
| 3 | 2.913E-03 |
| 3 | 6.005E-03 |
| 4 | 4.687E-03 |
| 5 | 5.568E-03 |
| 5 | 5.490E-03 |
| 6 | 2.272E-03 |
| 6 | 6.263E-03 |
| 7 | 4.155E-03 |
| 8 | 8.047E-03 |
| 8 | 5.939E-03 |
| 9 | 1.830E-03 |
| 9 | 7.722E-03 |
| 1 | 0.961E-02 |
| 1 | 0.951E-02 |
| 1 | 1.574E-02 |
| 1 | 2.129E-02 |
| 1 | 2.716E-02 |
| 1 | 3.307E-02 |
| 1 | 3.896E-02 |
| 1 | 4.485E-02 |

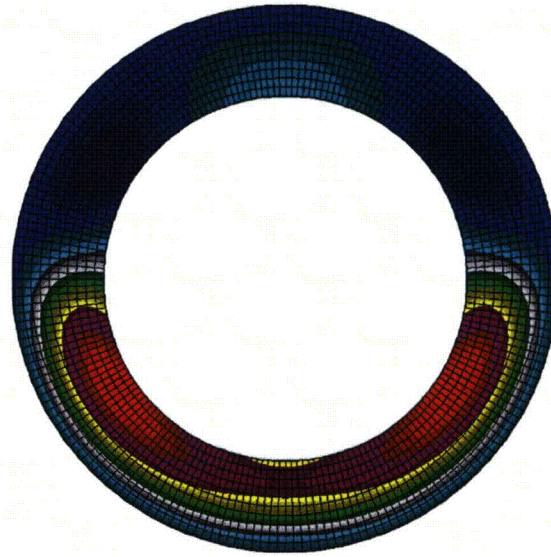


Figure 2-100. Lateral (Z) Displacement in Conical Shell – Model AOS-050

**2.12.13 Certificate of Conformance, General Plastics FR-3700 Series Foam –
AOS-165A Prototype**

THIS PAGE INTENTIONALLY LEFT BLANK



4910 Burlington Way, Tacoma, Washington 98409

T (253) 473.5000 F (253) 473.5104 TF (800) 806.6051 www.generalplastics.com

April 25, 2011

Alpha-Omega Services, Inc.
General Electric Nuclear Energy
6705 Vallecitos Road
Sunol, CA 95486

CORRECTED COPY

Attention: Receiving Quality Inspection

Subject: **CERTIFICATE OF CONFORMANCE**

Purchase Order #: **AOS-3835 Rev 2**

SJO Number: **5099-1**

Gentlemen:

This letter certifies that the **AOS-165** Impact Limiter filled with **LAST-A-FOAM® FR-3720** has been manufactured, tested and inspected in accordance with purchase order requirements. These products are classified "Safety Class A." Applicable drawings, specifications and standards called for by the purchase order:

Material Specs, Drawings and Process Standards:

105E9694 Rev. 3
22A9420 Rev. 1


Production control records and test reports covering subject material indicate conformance with applicable requirements and are attached.

Material: General Plastics Mfg. Co.'s
LAST-A-FOAM® FR-3720

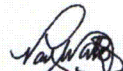
Quantity: 5 each **AOS-165 Units 01-05**

Respectfully submitted,

GENERAL PLASTICS MANUFACTURING COMPANY


Gerald Langston
Quality Engineer


GEH-NE Source Inspection 5/17/2011

 6-5-2011
ALPHA-Omega SERVICES INC. QA

- Enclosures:
- 5 each Production Control Records, Units 01-05.
 - 1 each Formulation Test report, LAST-A-FOAM® FR-3720 Batch # 243-CR04489 (Density, c/s, flame, intumescence, leachable chlorides, thermal conductivity, specific heat, water absorption, chemical composition), 19 pages total.
 - 1 each Batch Test Report, LAST-A-FOAM® FR-3720 Batch # 243-CR04489 (Density, c/s, flame, intumescence, leachable chlorides) 4 pages total.
 - General Plastics Reject Tag #'s 3095, 3099, 3109 & 3110.

THIS PAGE INTENTIONALLY LEFT BLANK

2.13 REFERENCES

- [2.1] U.S. Nuclear Regulatory Commission (NRC), *Title 10, Code of Federal Regulations, Part 71 (10 CFR 71)*, "Packaging and Transportation of Radioactive Material."
- [2.2] *International Atomic Energy Agency (IAEA) Safety Standards Series No. TS-R-1 (IAEA TS-R-1)*, "Regulations for the Safe Transport of Radioactive Material," 1996 Ed. (as amended 2003).
- [2.3] U.S. Nuclear Regulatory Commission (NRC), *Regulatory Guide 7.6*, "Design Criteria for the Structural Analysis of Shipping Cask Containment Vessels," Rev. 1, 1978.
- [2.4] U.S. Nuclear Regulatory Commission (NRC), *Regulatory Guide 7.8*, "Load Combinations for the Structural Analysis of Shipping Casks," Table 10, Rev. 1, 1989.
- [2.5] American Society of Mechanical Engineers, *ASME Boiler and Pressure Vessel Code*, Section II, Part D, 2004 Ed., No Addendum.
- [2.6] Gerard, George, *Introduction to Structural Stability Theory*, McGraw-Hill, New York, 1962, Equation 8-14, p. 142, and pp 143-146.
- [2.7] Kaminski, D. A., Ed., *Heat Transfer Data Book*, General Electric Company, New York, 1981, Section G515/29, p. 5.
- [2.8] American Society of Mechanical Engineers, *ASME Boiler and Pressure Vessel Code*, Section II, Part D, Table 3, p. 406, 2004 Ed., No Addendum.
- [2.9] D. Perry, *Aircraft Structures*, McGraw-Hill, 1950, pp. 398-400.
- [2.10] Metech Welded Mesh, Inc., Online Catalog, accessed June, 2010, <http://www.weldedwiremesh.net/>.
- [2.11] American National Standards Institute, *ANSI N14.5-1997*, "Radioactive Materials – Leakage Tests on Packages for Shipment," February 5, 1998.
- [2.12] MIL-STD-883B(3) NOT 2, "Dissimilar Metals," May, 1993.
- [2.13] General Plastics Manufacturing Company, *Design Guide for Use of LAST-A-FOAM FR-3700 for Crash & Fire Protection of Radioactive Material Shipping Containers*, Tacoma, WA, Issue 005.
- [2.14] ASME, Section III, Division 1, Appendices, Figure I-9.4, "Design Fatigue Curves for High Strength Steel Bolting for Temperatures Not Exceeding 700°F," 2004 Ed., No Addendum.
- [2.15] Caldwell, S.G., Ph.D., *Tungsten Heavy Alloy Engineering Manual*, ATI Firth Sterling, AL, v4.0.
- [2.16] Gibson, Lorna, J. and Michael F. Ashby, *Cellular Solids*, p. 193, Cambridge University Press, New York, NY, 2001.
- [2.17] Torrey Hills Technology, LLC, *High Density Tungsten Technical Data*, accessed September 19, 2010, <http://www.torreyhillstech.com/hddata.html>.
- [2.18] Lassner, Erik and Wolf-Dieter Schubert, *Tungsten – Properties, Chemistry, Technology of the Element, Alloys, and Chemical Compounds*, Kluwer Academic/Plenum Publishers, New York, NY, 1999.
- [2.19] General Plastics Manufacturing Company, *Design Guide for Use of LAST-A-FOAM FR-3700 for Crash & Fire Protection of Radioactive Material Shipping Containers*, Tacoma, WA, March, 1998 (revised October, 2003).

- [2.20] Communication from ATI Firth Sterling to Alpha-Omega Services, Inc., and GE Energy.
- [2.21] Parker O-Ring Division, *Evaluation of Parker Compound S1224-70 to ASTM D2000 7GE705 A19 B37 EA14 EO16 E036 F19 G11 Compound Data Sheet*, Kentucky, June 19, 1996.
- [2.22] Fitzroy, Nancy D., Ed., *Heat Transfer Data Book*, General Electric Company, New York, November, 1970 Edition, Section G502.5, p. 7.
- [2.23] Touloukian, Y. S., *Thermophysical Properties of Matter, Metallic Elements and Alloys*, 1971.
- [2.24] Fischer, L. E. and W. Lai, *NUREG/CR-3854, Fabrication Criteria for Shipping Containers*, Lawrence Livermore Laboratory, Prepared for U.S. Nuclear Regulatory Commission (NRC), Livermore, California, March, 1985.
- [2.25] Monroe, R. E., H. H. Woo, and R. G. Sears, *NUREG/CR-3019, Recommended Welding Criteria For Use in the Fabrication of Shipping Containers for Radioactive Materials*, Lawrence Livermore Laboratory, Prepared for U.S. Nuclear Regulatory Commission (NRC), Livermore, California, March, 1984.
- [2.26] American Society of Mechanical Engineers, *ASME Boiler and Pressure Vessel Code, Section III, Division 1, Subsection NB*, 2004 Ed., No Addendum.
- [2.27] ASTM International, *ASTM F1145 - 05(2011), Standard Specification for Turnbuckles, Swaged, Welded, Forged*, Table 3, West Conshohocken, PA, 2011.
- [2.28] Shigley, Joseph E., *Mechanical Engineering Design*, Chapter 6, "The Design of Screws, Fasteners, and Connections," McGraw Hill, Inc., 3rd Edition, 1977.